Optimized Codebook Based Hybrid Beamforming

Juan Vidal Alegría
juan.vidal.alegria@gmail.com
ju4855vi-s@student.lu.se

Department of Electrical and Information Technology
Lund University

Supervisor: Ove Edfors

Examiner: Fredrik Rusek

December 17, 2018

Printed in Sweden
Tryckeriet i E-huset, Lund

Abstract

In this thesis we research beamforming capabilities of the UEs equipped with several antennas in a 5G scenario.

We define a system model based on the use of phase codebooks that allow to change the radiation patterns of the arrays of antennas installed in the UE. Within this system model, we obtain optimized codebooks in terms of two metrics, which we consider to be of interest in this scenario, employing two different optimization approaches. We use these results to analyze, through simulations, the estimation performance in an AoA estimation scenario. We also analyze the detection performance in receiving the signal that can allow us to estimate the AoA.

So as to gain more insight into how the selection of the optimum codebook affects the detection performance, we define a simpler scenario and we analyze it theoretically and draw conclusions that relate to the simulations obtained.

Popular Science Summary

When you think about mobile phones nowadays, no one thinks about the old devices with small screens that you may still keep in a drawer full of dust in the basement of your home. Those devices could be used to make phone calls, maybe they could even send SMSs, and, if you were lucky, you could even use them to play some simple games, such as "Snake" or "Tetris", that required no internet connection. They were the only mobile phones available around 20 years ago. Nowadays, however, one cannot think of a mobile phone without internet connection to use social media or stream videos or music.

If we think about the original functionalities of mobile phones, i.e., phone calls and SMSs, they are just minor features in the new mobile phones (or smartphones) that are getting substituted by apps running directly through the internet connection. In addition, the number of devices connected to the mobile network is increasing at huge rates, not only more people have access to smartphones now (some people even have more than one), but also new devices are getting connected to this network including tablets, TVs, cars, sensors... All these devices require high data rates to run their services smoothly, and with the current networks it's getting harder and harder to be able to serve those data rates. This is one of the main reasons for the development of 5G, the next generation of mobile communications that will come to solve the increasing need of high data rates as well as other issues related.

Many technologies are being considered to improve the data rates in 5G. Some include putting a lot of antennas in the base stations, putting a lot of base stations to serve smaller areas, or using new frequency bands that are highly unoccupied. In the current generation of mobile communications, i.e. 4G, one of the improvements with respect to the previous generation to get higher data rates was to put several antennas in the smartphones or, in general, any device that is to be connected to the mobile network. Thus, in 5G we expect to have smartphones with several antennas, probably even more than in 4G, so that we can still take benefit of them. However, the way the base stations will work in 5G is quite different to the way they used to do in 4G. This means that we will have to think again how can we take benefit from the use of different antennas in the 5G devices. In this thesis we will propose some methods to utilize the antennas in these devices in a 5G scenario and study what benefits can we get from them.

List of Acronyms and Abbreviations

AoA - Angle of Arrival

AWGN - Additive White Gaussian Noise

BS - Base Station

CRLB - Cramer Rao Lower Bound

MA - Multiple Antenna

DOA - Direction Of Arrival

GLRT - Generalized Likelihood Ratio Test

LOS - Line Of Sight

ML - Maximum Likelihood

MLE - Maximum Likelihood Estimator

MRC - Maximum Ratio Combining

MSE - Mean Squared Error

P_{D} - Probability of Detection

PDF -Probability Density Function

P_{FA} - Probability of False Alarm

RF - Radio Frequency

ROC - Receiving Operating Characteristic

SNR - Signal to Noise Ratio

UE - User Equipment

Table of Contents

List of Figures

List of Tables

Chapter 1
Introduction

Mobile communications technology is evolving quickly. The demand for high data rates and low latencies, to comply with the new services being deployed, is increasing and will soon be impossible to meet with the current infrastructure. In addition, new emerging services are being developed with requirements in terms of reliability, number of devices connected, etc, that cannot be fulfilled by the current mobile communication systems. All these factors, together with the increasing number of new devices getting connected everyday [1, 2] are forcing the standardization bodies, and the wireless communications industry in general, to work towards a new generation of cellular mobile communications. 3GPP has already delivered the first set of 5G standards in its release 15 [3] and is currently working on the next Release.

In this thesis we will be looking at the physical layer of the next generation 5G systems. More specifically, we will focus on the UE side, and explore how to exploit the beamforming capabilities available in this side.

1.1 Technical Background

In [2] an overview of the major requirements for 5G systems is exposed. We will put the focus on the high data rates requirement since it can be seen as one of the most challenging requirements, and most of the advances in this requirement come from improvements in the physical layer. The main technologies that are being explored to fulfill this requirement are [1] the densification and offloading by deploying more cells with smaller service areas, the exploitation of the high bandwidths available in the millimeter-wave spectrum, and the use of massive MIMO to improve the bandwidth efficiency through spatial multiplexing.

> **Densification.** This strategy consists of the use of small cells, i.e., cells that cover a smaller area by utilizing low power access nodes. These small cells allow to reuse the spectrum more efficiently and they reduce the number of users sharing resources from a BS. This leads to a gain in the effective data rates when the interference between cells is low enough [1], which is the usual scenario, specially considering the mm-wave spectrum.
>
> Regarding the influence of densification in channel modeling, which will be of interest for the subsequent chapters, we expect that the probability

of having a LOS component increases since the users will be closer to the access nodes.

Millimeter-Wave. Millimeter-wave spectrum is the band of spectrum between 30 and 300 GHz. This band has been historically avoided for mobile communications mainly due to the hostile propagation conditions and the lack of cost-effective technology available for this band. However, the sub-3 GHz spectrum is getting too crowded to fit the bandwidths needed for the high data rates demanded and the growing number of devices connected. On the other hand, a great part of the mm-wave spectrum remains unused, which means that there is a huge amount of bandwidth available in this band which could be used to increase the data rates and fit more users in new mobile communication systems. Therefore, this band is being considered and research is being conducted to be able to use this band for the next generation 5G systems [4].

The channel characteristics in a mm-wave scenario are significantly different to the ones in the sub-3 GHz band due to the propagation peculiarities of mm-waves. The penetration of these waves through walls and buildings is low, so indoor networks would be highly isolated from outdoor networks [4]. When the transmission is highly directive, the propagation characteristics associated to this band causes the received signals to arrive at a few main AoAs, even if there is no LOS component [5].

Massive MIMO. Multiuser MIMO consists of a BS with a certain number of antennas communicating with one or more UEs. Massive MIMO is an extension over multiuser MIMO in which the number of antennas at the BS is large compared to the number of UEs communicating with it. This way it can spatially focus the energy to each UE, allowing spatial multiplexing, and thus, improving the throughput [6].

Massive MIMO can concentrate the power towards specific directions of the space, obtaining extremelly narrow beams. Then, if we consider the use of massive MIMO at millimeter waves frequencies [7], together with a densified network, many of the multipath components are eliminated. This way we can think of a quasi-LOS channel model, where we have a strong signal arriving at a certain AoA to the UE.

A lot of research has been already conducted in these three technologies. In most scenarios, specially if we look at the massive MIMO original scenario [8], the UE is assumed to have a single antenna. However, since the release of LTE by 3GPP, the UEs that have been developed included several antennas to be able to operate in the different MIMO transmission modes defined for LTE [9]. Furthermore, some of the proposed designs for the next generation devices include several beamforming modules consisting of phased arrays with several antennas in a certain configuration, such as 4×2 [10]. If we look at the technical specifications for the 5G UE, still being written by 3GPP, we can also see that the UEs in 5G will be able to operate using several antennas [11]. The way in which the antennas at the UE are used in a 5G scenario is still a matter of research and will be our focus throughout this thesis.

In [12], beamforming for UE discovery is studied, but in this scenario a simple MIMO system is considered. We will research beamforming capabilities of the antennas equipped in the UEs without interacting directly with the massive MIMO algorithms that will operate on top of that. To do so, we will assume a quasi-LOS channel with a main AoA, as a result of using the three technologies mentioned before, and a UE with several antennas that can only use a finite number of phase shifts for the beamforming. All the antennas receive in the end a single digital value, but there are individual phase rotations at each antenna. This is customary called hybrid beamforming [13].

1.2 Objectives

The aim of this master's thesis is to study the beamforming capabilities of the UEs in a 5G scenario. We want (1) to define a codebook approach for controlling the beamforming parameters of the UE, (2) to obtain optimum codebooks through different methods considering this approach, and (3) to analyze the performance of these optimized codebooks in different situations. To do so we will have to make use of optimization and simulation tools, as well as theoretical analysis. It is our goal to be able to get closed form results out of the theoretical analysis so that they can be compared to some extent with the simulation results.

1.3 Thesis Outline

After Chapter 1, where we have introduced the main topic of the thesis and the related information, we have three main chapters. Chapter 2 introduces the main system model and shows the results of optimizing the beamforming characteristics of the UE with repect to two metrics of interest. In Chapter 3, results from Chapter 2 are used in a similar scenario, where in this case the problem considered is to estimate the AoA of an incoming signal at the UE, and simulation results are exposed to compare the performance of the different optimization approaches. Chapter 4 presents a new simplified scenario to be able to explain theoretically the detection performance simulated in Chapter 3 for the different optimization approaches. The last chapter provides the conclusions reached after doing this thesis and suggestions for future work that can be done in this topic.

1.4 Limitations

Throughout this thesis we consider a theoretical scenario which in reality would have certain limitations:

- We don't consider any interference coming from adjacent base stations. This would limit the performance of the system considered since the optimum phase codebooks may radiate outside the area of interest, capturing the interference.

- We are not considering the radiation pattern of the antenna elements conforming the array. This patter could influence the results of the optimized codebooks.
- The phase values of the optimized codebooks can take any continuous values. In reality, however, they are limited to have a certain resolution.
- We consider ideal noise. If there was some correlation between noise samples the results may change.

Chapter 2

Multiple-Antenna User Equipment Beamforming Optimization

In this chapter an optimization of the beamforming capabilities of a multiple-antenna UE with respect to two performance metrics is presented. These metrics are meant to increase the received power in the scenario defined and they will be further analyzed. The results obtained from the optimization, as well as the scenario that is presented, will be taken into account and analyzed more closely in the subsequent chapters.

2.1 System Model

A receiving UE with a linear antenna array of N antenna elements is considered. Each antenna element is equipped with a phase shift module. The antenna element spacing is assumed to be half a wavelength and the antenna elements to be placed in a straight line. In this scenario, an incident signal forming an angle ϑ with the antenna array is received as

$$\boldsymbol{z} = \boldsymbol{a}(\vartheta)x + \boldsymbol{n}, \tag{2.1}$$

where x corresponds to a transmitted symbol, $\boldsymbol{n}$ is AWGN, and $\boldsymbol{a}(\vartheta)$ is the array response in the direction ϑ, which can be expressed as [14]

$$\boldsymbol{a}(\vartheta) = \begin{bmatrix} 1 & e^{j\pi\sin(\vartheta)} & \dots & e^{j\,N\pi\sin(\vartheta)} \end{bmatrix}^T. \tag{2.2}$$

The post-processed signal after the phase shift module is

$$y = F(\vartheta)x + \tilde{n}, \tag{2.3}$$

where $F(\vartheta)$ is defined as the array factor [14], and $\tilde{n}$ is again AWGN. The array factor is a weighted sum of the array response for each antenna element. The array factor in our scenario, as defined in Figure 2.1, for an angle of arrival (AoA) $\vartheta \in [-\pi/2, \pi/2]$, is given by

$$F(\vartheta) = \boldsymbol{w}^T\boldsymbol{a}(\vartheta), \tag{2.4}$$

where $\boldsymbol{w}$ collects the tunable complex phase shifts for each antenna element

$$\boldsymbol{w} = \begin{bmatrix} e^{j\varphi_1} & e^{j\varphi_2} & \dots & e^{j\varphi_N} \end{bmatrix}^T, \tag{2.5}$$

and $\varphi_k \in [0, 2\pi]$. Note that, in this definition, $\boldsymbol{w}$ is not normalized, so that $\tilde{n}$ has variance N times the variance of n_n. However, this won't affect the results in this chapter, and we can consider a scaling factor of $\frac{1}{\sqrt{N}}$ for $\boldsymbol{w}$ if we want to avoid this fact. The array gain definition that we will use is

$$G(\vartheta) = |F(\vartheta)|^2 = \boldsymbol{w}^T \boldsymbol{a}(\vartheta) \boldsymbol{w}^H \boldsymbol{a}^*(\vartheta). \tag{2.6}$$

If we restrict $\boldsymbol{w}$ to the form (2.5) so that the power is constrained, $G(\vartheta)$ is maximized when $\boldsymbol{w} = \boldsymbol{a}^*(\vartheta)$, which corresponds to setting $\varphi_n = n\pi \sin(\vartheta)$. However, in reality, the vector $\boldsymbol{w}$ can only be chosen from a limited set. In our scenario we will have a limited number L of phase combinations, i.e., the vector $\boldsymbol{w}$ can only be chosen from a closed set $\{\boldsymbol{w}_l\}_{l=1}^{L}$, here denoted as codebook, where

$$\boldsymbol{w}_l = \begin{bmatrix} e^{j\varphi_{1,l}} & e^{j\varphi_{2,l}} & ... & e^{j\varphi_{N,l}} \end{bmatrix}^T \tag{2.7}$$

corresponds to a codeword, which gives an array gain $G_l(\vartheta)$ in the direction ϑ. This means that the phase shift modules will take values $\{\varphi_{1,l}, ..., \varphi_{N,l}\} \in [0, 2\pi]^N, l = 1, ..., L$.

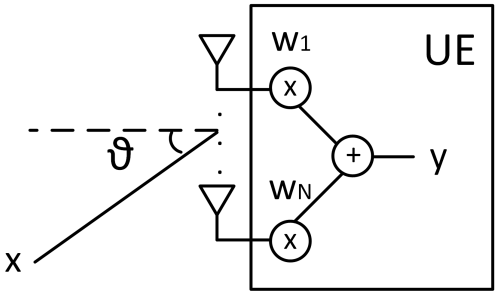

Figure 2.1: Block diagram of the UE.

In this chapter we will focus on obtaining optimum codebooks, in terms of the two performance metrics that we will define, for different values of L and N. The combination of the array gains for all the $\boldsymbol{w}_l$ of a codebook for all the directions of the space considered can be associated to a total array gain for that codebook

$$G_{\mathrm{T}}(\vartheta) = \max_{l \in [1,L]} G_l(\vartheta) = \max_{l \in [1,L]} \boldsymbol{w}_l^T \boldsymbol{a}(\vartheta) \boldsymbol{w}_l^H \boldsymbol{a}^*(\vartheta). \tag{2.8}$$

Two metrics will be considered to determine how good a finite codebook can perform with respect to a pure MRC approach: the average loss and the maximum loss. We will discuss these two criteria next. Figure 2.2 shows a graphical aid to these metrics.

2.1.1 Average loss

By average loss we mean the average loss of the total array gain $G_{\mathrm{T}}(\vartheta)$ with respect to the MRC array gain throughout all the directions of the space considered Ω,

where we will assume the incoming angle to be uniformly distributed in Ω. We express the average loss in dB and define it formally as

$$L_{\text{avg}} = 10 \log_{10} \left(\frac{1}{S_\Omega} \int_\Omega \frac{G_{\text{MRC}}}{G_{\text{T}}(\vartheta)} \mathrm{d}\vartheta \right), \tag{2.9}$$

where S_Ω is the size of the space considered, which we for simplicity express in degrees from now (and similarly for ϑ), and G_{MRC} is the array gain obtained when using MRC

$$G_{\text{MRC}} = \boldsymbol{a}^H \boldsymbol{a}(\vartheta) \boldsymbol{a}^T \boldsymbol{a}^*(\vartheta) = N^2, \tag{2.10}$$

which depends only on the number of antennas and could be scaled if a different reference amplitude is considered.

2.1.2 Maximum loss

By maximum loss we mean the maximum loss of the total array gain $G_{\text{T}}(\vartheta)$ with respect to the MRC array gain. It will also expressed in dB scale and computed as

$$L_{\text{max}} = \max_{\vartheta \in \Omega} \left[10 \log_{10} \left(\frac{G_{\text{MRC}}}{G_{\text{T}}(\vartheta)} \right) \right]. \tag{2.11}$$

For the definition of the physical space we will assume that the antenna array of the UE is placed along the X axis. If we consider the spherical coordinates ϕ and θ, for $\phi = 0$, ϑ would correspond directly to the spherical coordinate θ. Three possible ranges will be used for this θ coordinate, $\Omega_{60^\circ} = [-30^\circ, 30^\circ]$, $\Omega_{100^\circ} = [-50^\circ, 50^\circ]$ and $\Omega_{140^\circ} = [-70^\circ, 70^\circ]$. This will let us observe the effects of changing the width of the space considered, i.e., S_Ω, in the results obtained. Intuitively, the narrower the space we consider, the lower codebook size, L, will be needed to obtain good results for L_{avg} and L_{max}. In a real scenario, the space is limited by the beamwidth of the radiating element of the array, so since we consider a collection of widths, our results can cover various antenna element implementations.

In the case of a 2D array, the array will be positioned in the XY plane, and the incoming angle would correspond to a combination of the spherical coordinates θ and ϕ. Our analysis can be extended directly by adopting the formulation of the array response accordingly. In this case the θ range considered will be the same as in the previous one, but for ϕ we will consider the full range, $\phi \in [0, 180]$.

2.2 Optimization

An ideal codebook would be the one that simultaneously minimizes both metrics L_{avg} and L_{max}. However, it is not intuitive whether both metrics can be simultaneously minimized and we can expect that there would be an optimum operating region instead. In other words, the optimal codebooks may be attained by a carefully chosen trade-off between L_{avg} and L_{max}.

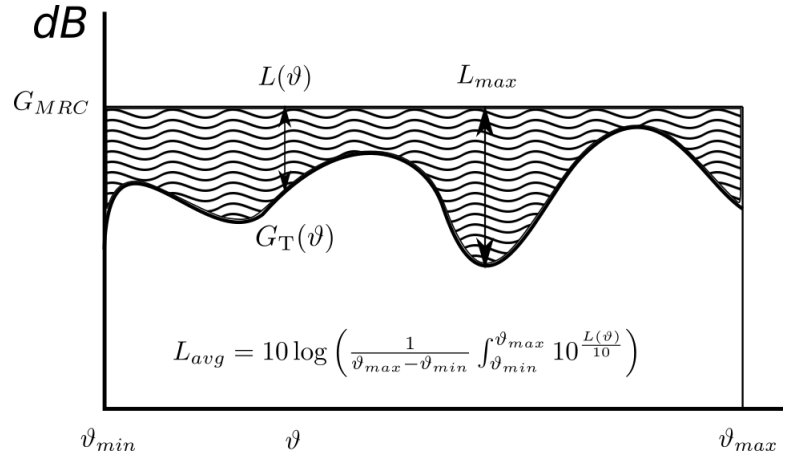

Figure 2.2: Performance metrics defined.

2.2.1 Steering optimization

The first approach would be to use $\boldsymbol{w}_l = \boldsymbol{a}^*(\vartheta_l)$ and find the optimum set of $\{\vartheta_l\}_{l=1}^L$ that minimizes L_{avg} for a given value of L_{max}. This physically means to select a set of angles where the MRC approach will be applied, in case the received signal comes from those directions, to optimize the total array gain in the space considered. In array synthesis it would correspond to steer the main lobe of the radiation pattern towards specific directions defined by $\{\vartheta_l\}_{l=1}^L$. So the optimization problem would be

$$\min_{\{\vartheta_l\}_{l=1}^L} L_{\mathrm{avg}} = \frac{1}{S_\Omega}\int_\Omega \frac{G_{\mathrm{MRC}}}{G_{\mathrm{T}}(\vartheta)}\mathrm{d}\vartheta \tag{2.12a}$$

$$s.t.\, L_{\mathrm{max}} = \alpha, \tag{2.12b}$$

where α is the desired L_{max} value, and in this case

$$G_{\mathrm{T}}(\vartheta) = \max_{l\in[1,L]} \boldsymbol{a}^H(\vartheta_l)\boldsymbol{a}(\vartheta)\boldsymbol{a}^T(\vartheta_l)\boldsymbol{a}^*(\vartheta). \tag{2.13}$$

This optimization approach is restricted by the fact that only specific values of $\boldsymbol{w}_l$ are considered, so this can limit the performance of the system. Also, the more antennas available at the UE, the narrower the main lobe of the radiation pattern, thus a greater L would be needed to obtain a good performance. However, this is the most common approach due to its physical simplicity—it can be as simple as to divide the space into L sections and define each $\boldsymbol{w}_l$ to point to one section.

The optimization problem is unfeasible to solve in closed form, so several numerical optimization methods have been tried, obtaining poor results. Therefore, the algorithm used in the end consists of a random search, in which we use at least 10^7 iterations. Each iteration would give a value of the pair L_{avg}, L_{max} by randomly choosing $\{\vartheta_l\}_{l=1}^L$. We will store only the optimum $\{\vartheta_l\}_{l=1}^L$ in terms of L_{avg} for every possible value of L_{max} in a grid with 0.1dB spacing. All the possible combinations L_{avg} and L_{max} obtained will also be stored to be able to

observe the possible operating area. In Algorithm 1 we provide pseudocode for this optimization algorithm.

Algorithm 1 Pseudocode for the steering optimization algorithm.

for $i = 1 \rightarrow 10^7$ **do**
    get random $\{\vartheta_l\}_{l=1}^{L}$
    compute L_{avg} & $L_{\max}$
    $L(i,1) \leftarrow L_{\text{avg}}$
    $L(i,2) \leftarrow L_{\max}$
    $R(i) \leftarrow \{\vartheta_l\}_{l=1}^{L}$
for $\alpha = 0 \rightarrow \infty$ with steps of 0.1 **do**
    $n_\alpha = \arg\min_i L(i,1),\ s.t.\, L(i,2) = \alpha$
    Save $\{\vartheta_l\}_{l=1}^{L} = R(n_\alpha)$

2.2.2 Pure phase optimization

The second approach would be to consider any possible combination of phases for every codeword $\boldsymbol{w}_l$. In the worst case, this optimization would give the same solution as the steering optimization since it includes the cases where $\boldsymbol{w}_l = \boldsymbol{a}^*(\vartheta_l)$. The optimization can be then formulated as

$$\min_{\{\varphi_{1,l},\ldots,\varphi_{N,l}\}_{l=1}^{L}} L_{\text{avg}} = \frac{1}{S_\Omega}\int_\Omega \frac{G_{\text{MRC}}}{G_{\text{T}}(\vartheta)}\mathrm{d}\vartheta \tag{2.14a}$$

$$s.t.\, L_{\max} = \alpha, \tag{2.14b}$$

where we can see that the only thing that changes with respect to the previous case is that $G_{\text{T}}(\vartheta)$ corresponds to (2.8), where $\{\varphi_{1,l},...,\varphi_{N,l}\}_{l=1}^{L}$ has no restrictions, i.e., $\varphi_{n,l}$ can take any number between 0 and 2π. We will assume anyway that $\varphi_{1,l} = 0$ in all the codewords without losing any generality, since the only thing that matters is the phase variation between the antennas and we can take the first antenna as phase reference.

The optimization algorithm consists also in a random search with the same considerations as in Section 2.2.1, but in this case we will use a number of iterations according to the number of possible variables and the available time for the project. This number must be much bigger than in the case of steering optimization since the search space is vastly expanded, but we have been constrained by the time limitation of the project and the results could be more accurate if a more exhaustive optimization is used. In case worse results than the steering optimization are obtained, we assume equal results since the pure phase optimization is a more general case and its optimum results must be at least as good as in steering optimization. In Algorithm 2 we provide pseudocode for this optimization algorithm.

Algorithm 2 Pseudocode for the pure phase optimization algorithm.

for $i = 1 \rightarrow 10^8$ (or more) **do**
    get random $\{\varphi_{1,l}, ..., \varphi_{N,l}\}_{l=1}^{L}$
    compute L_{avg} & $L_{\max}$
    $L(i,1) \leftarrow L_{\text{avg}}$
    $L(i,2) \leftarrow L_{\max}$
    $R(i) \leftarrow \{\vartheta_l\}_{l=1}^{L}$
for $\alpha = 0 \rightarrow \infty$ with steps of 0.1 **do**
    $n_\alpha = \arg\min_i L(i,1),\ s.t.\ L(i,2) = \alpha$
    Save $\{\varphi_{1,l}, ..., \varphi_{N,l}\}_{l=1}^{L} = R(n_\alpha)$

2.3 Results

In this section the results of the optimization problems defined previously are presented. For the simulation we have considered a spacing of 1° in the θ coordinate, and 2° in the ϕ coordinate for the 2D arrays. The precision considered for the results of L_{avg} and $L_{\max}$ is 0.1dB.

Table 2.1 contains all the optimum values obtained in terms of L_{avg} and $L_{\max}$ for all the combinations considered. If we look at these results we notice that in some cases the steering optimization can perform as good as the pure phase optimization. In the simulations they could actually be worse due to the time limitations of the project, which made the number of iterations in the pure phase optimization in some cases insufficient to obtain the optimum results. This happens specially when the range considered is not wide enough compared to the beam width times the codebook size L, where both optimization results should converge. Also, the greater the number of phase variables, i.e. more antennas or higher L, the worse the performance of the random search optimization since the number of possible combinations grows exponentially. To get more accurate results, a higher number of iterations should be used, or a better optimization method should be derived.

In general, the pure phase optimization can get much better results than steering optimization both in terms of L_{avg} and $L_{\max}$, but specially in the latter, when working with a low L and/or a wide range. Furthermore, this optimization approach gives more freedom in choosing the operating region as a compromise between L_{avg} and $L_{\max}$ since it allows to change the shape of the main lobes as well as their steering angles.

In Figures 2.3-2.7 we can observe some examples where the pure phase optimization yields better results than the steering optimization. As we could expect, in most of the cases there is not an optimum operating point since in general the point where $L_{\max}$ is minimum doesn't correspond to the point where L_{avg} is minimum. Instead, we can see that the interesting operating region is given by the line relating the minimum L_{avg} and the minimum $L_{\max}$.

In the next chapters we will focus on the results for 4×1 configuration with $L = 2$ codewords and in the range $\Omega_{140°}$. This is mainly because it is the simplest use

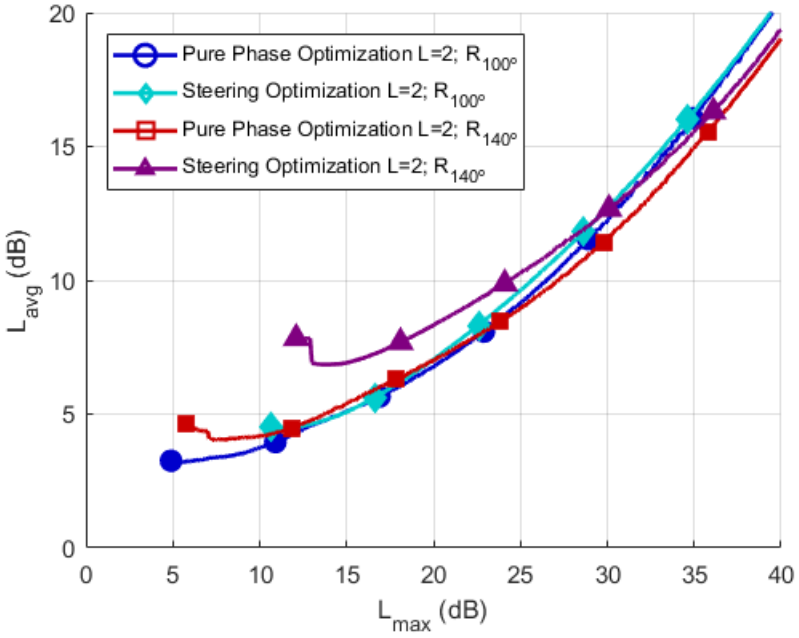

Figure 2.3: 4x1 antenna configuration, $L = 2$.

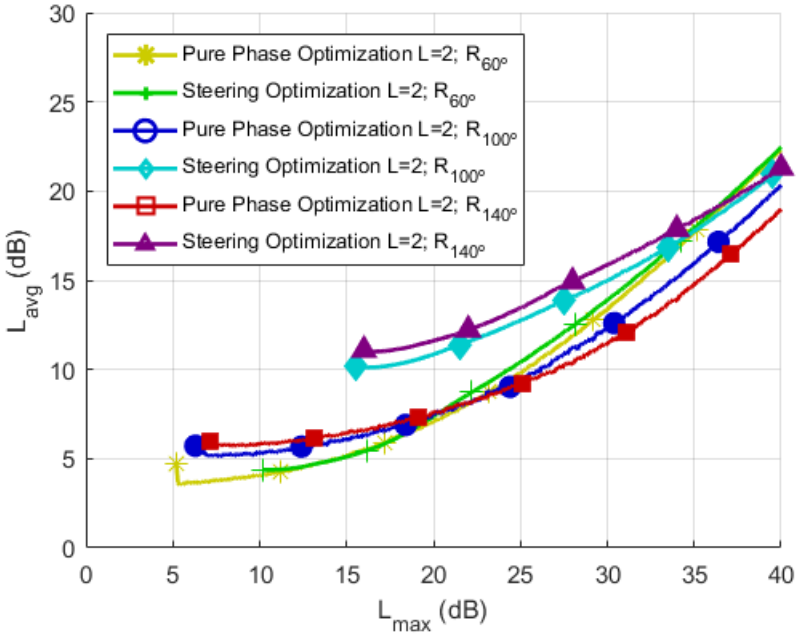

Figure 2.4: 6x1 antenna configuration, $L = 2$.

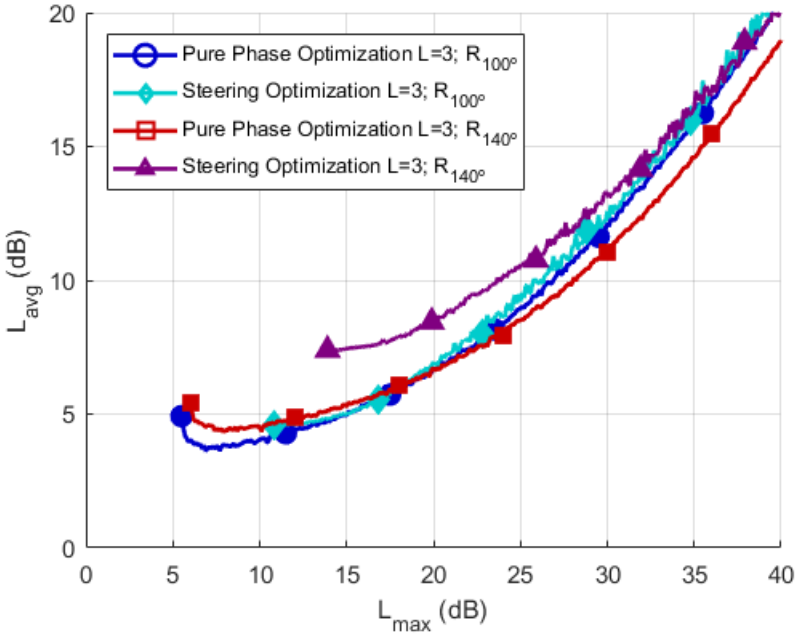

Figure 2.5: 6x1 antenna configuration, $L = 3$.

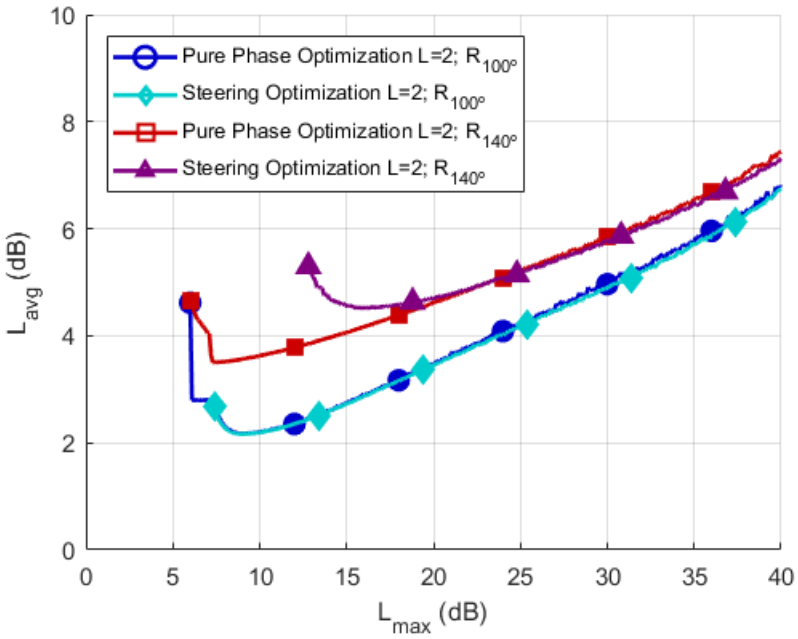

Figure 2.6: 2x2 antenna configuration, $L = 2$.

Table 2.1: Optimum results 1D arrays (in bold the values of the metrics that are optimum for each configuration).

	Ω_{60°		Ω_{100°		Ω_{140°	
	$L_{\text{avg}}(dB)$	$L_{\text{max}}(dB)$	$L_{\text{avg}}(dB)$	$L_{\text{max}}(dB)$	$L_{\text{avg}}(dB)$	$L_{\text{max}}(dB)$
	4x1 Pure Phase Optimization. Optimum L_{avg}.					
$L=2$	**1.4**	3.8	**3.2**	5.6	**4**	7.4
$L=3$	**0.6**	**1.5**	**1.4**	4.1	**2.4**	6.9
$L=4$	**0.3**	**0.9**	**0.7**	**2.1**	**1.2**	**3.2**
	4x1 Pure Phase Optimization. Optimum L_{max}.					
$L=2$	2.1	**3.6**	3.3	**4.9**	4.6	**5.8**
$L=3$	**0.6**	**1.5**	2.7	**3.4**	2.7	**4.4**
$L=4$	**0.3**	**0.9**	**0.7**	**2.1**	**1.2**	**3.2**
	4x1 Steering Optimization. Optimum L_{avg}.					
$L=2$	**1.4**	3.7	4.5	10.6	6.8	13.7
$L=3$	**0.6**	**1.5**	**1.4**	4.1	**2.4**	6.9
$L=4$	**0.3**	**0.9**	**0.7**	**2.1**	**1.2**	**3.2**
	4x1 Steering Optimization. Optimum L_{max}.					
$L=2$	**1.4**	3.7	4.5	10.6	7.8	12.1
$L=3$	**0.6**	**1.5**	1.5	3.8	2.5	6.1
$L=4$	**0.3**	**0.9**	**0.7**	**2.1**	**1.2**	**3.2**
	6x1 Pure Phase Optimization. Optimum L_{avg}.					
$L=2$	**3.5**	5.4	**5.1**	7.7	**5.7**	9.3
$L=3$	**1.4**	3.7	**3.6**	6.9	**4.3**	7.9
$L=4$	**0.7**	**2.2**	**2**	5.5	**3.4**	8.7
	6x1 Pure Phase Optimization. Optimum L_{max}.					
$L=2$	4.7	**5.2**	5.7	**6.3**	6	**7.1**
$L=3$	2.9	**3.4**	4.9	**5.5**	5.4	**6**
$L=4$	**0.7**	**2.2**	3.5	**4.9**	4.2	**5.5**
	6x1 Steering Optimization. Optimum L_{avg}.					
$L=2$	4.4	10.2	10.1	16.1	11	16.3
$L=3$	**1.4**	3.7	4.6	10.8	7.4	13.9
$L=4$	**0.7**	**2.2**	**2**	5.5	3.5	10.1
	6x1 Steering Optimization. Optimum L_{max}.					
$L=2$	4.4	10.2	10.2	15.5	11.1	16
$L=3$	**1.4**	3.7	4.6	10.8	7.4	13.9
$L=4$	**0.7**	**2.2**	**2**	5.5	3.6	9

Table 2.2: Optimum results 2D arrays (in bold the values of the metrics that are optimum for each configuration).

	Ω_{60°		Ω_{100°		Ω_{140°	
	$L_{\text{avg}}(dB)$	$L_{\max}(dB)$	$L_{\text{avg}}(dB)$	$L_{\max}(dB)$	$L_{\text{avg}}(dB)$	$L_{\max}(dB)$
	2x2 Pure Phase Optimization. Optimum L_{avg}.					
$L=2$	**0.7**	3.3	**2.2**	9	**3.5**	7.3
	2x2 Pure Phase Optimization. Optimum $L_{\max}$.					
$L=2$	1	**2.8**	4.6	**6**	4.7	**6**
	2x2 Steering Optimization. Optimum L_{avg}.					
$L=2$	**0.7**	3.3	**2.2**	9	4.5	15.9
	2x2 Steering Optimization. Optimum $L_{\max}$.					
$L=2$	1	**2.8**	2.7	7.4	5.3	12.8
	4x2 Pure Phase Optimization. Optimum L_{avg}.					
$L=2$	**1.7**	**5.5**	**4.8**	11	**6.5**	10.9
	4x2 Pure Phase Optimization. Optimum $L_{\max}$.					
$L=2$	**1.7**	**5.5**	6.5	**8.6**	7.1	**9.8**
	4x2 Steering Optimization. Optimum L_{avg}.					
$L=2$	**1.7**	**5.5**	5.5	16.8	10.1	27.5
	4x2 Steering Optimization. Optimum $L_{\max}$.					
$L=2$	**1.7**	**5.5**	7.2	15.4	11	21.4

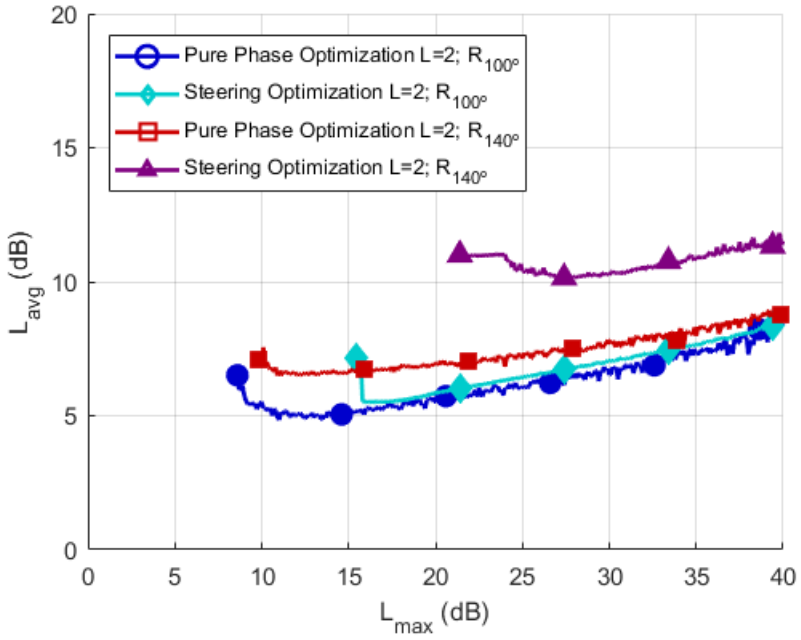

Figure 2.7: 4x2 antenna configuration, $L = 2$.

case where a great improvement can be achieved by using pure phase optimization instead of steering optimization, both in terms of L_{avg} and L_{max}.

2.4 Concluding Remarks

In this chapter we have defined the system model, using a codebook approach for hybrid beamforming in UEs, that will be the basis of this thesis. We have also obtained optimum phase codebooks in terms of L_{avg} and L_{max}. We have observed that, in general, L_{avg} and L_{max} cannot be simultaneously maximized, and that, in most of the cases, the pure phase optimization method offers a better operating region than the steering optimization method, i.e., with more freedom to choose the optimum values of L_{avg} and L_{max}. At this point we have resolved the two first parts of our objectives.

Chapter 3
Angle of Arrival Estimation

In the previous chapter we have obtained some interesting results from optimizing the phase codebooks with respect to two simple performance metrics. We would like to go a bit further with these results and understand what practical improvements we can get by using the pure phase optimization results compared to using the steering optimization results as well as the influence on AoA estimation of each of the defined metrics.

3.1 System Model

In this chapter we will follow the same model as in the previous chapter for the UE. We will focus on the case where the UE has a linear array for receiving, and more specifically we will only analyze the case where this array is a 4x1 array in the range Ω_{140° and the codebook size L is equal to 2. This is mainly because it is a simple case and the results are interesting when exploring the tradeoff between the two performance metrics that have been optimized.

In this case, we will put our focus on the AoA (or DOA) estimation using the results from the previous chapter. This is a common use case that is of interest both in terms of positioning [15, 16], and in terms of minimizing the pointing losses between the UE and the BS [17]. We will study how the results from the Chapter 2 affect AoA estimation.

We will assume that a pilot signal is transmitted from the BS to the UE. Taking the narrowband assumption [18], and considering the same scenario described in Figure 2.1, the arriving signal at the UE can be seen as just a "1" multiplied by the array response plus noise. So we would have an incoming signal at timeslot l

$$\boldsymbol{z}_l(\vartheta) = \boldsymbol{a}(\vartheta) + \boldsymbol{n}_l, \tag{3.1}$$

where $\boldsymbol{a}(\vartheta)$ is defined as in (2.2) with $N = 4$ in this case (the vector $\boldsymbol{z}_l$ has therefore size $N \times 1$), ϑ corresponds to the AoA that we want to estimate, and $\boldsymbol{n}_l$ is complex AWGN distributed as

$$\boldsymbol{n}_l \sim \mathcal{CN}\left(\boldsymbol{0}, N_0 \boldsymbol{I}\right). \tag{3.2}$$

Each of the phase codewords inside the desired phase codebook from the ones obtained in the previous chapter will be applied to this signal, taking as many timeslots there are codewords in the codebook (in this case we are interested the

size $L = 2$). Note that the same signal is transmitted over the L timeslots and ϑ is assumed to be constant over these timeslots. This will give an equivalent received signal

$$\boldsymbol{y} = \boldsymbol{W}^T \boldsymbol{a}(\vartheta) + \tilde{\boldsymbol{n}}, \tag{3.3}$$

where $\boldsymbol{W}$ is the matrix associated to a whole codebook using the codewords $\boldsymbol{w}_l$ from (2.7) as columns and normalizing so as not to increase the noise

$$\boldsymbol{W} = \left[\frac{\boldsymbol{w}_1}{\sqrt{N}} \ \frac{\boldsymbol{w}_2}{\sqrt{N}} \ ... \ \frac{\boldsymbol{w}_L}{\sqrt{N}} \right], \tag{3.4}$$

where $L = 2$ and $N = 4$. Note that the new noise vector has elements of the form

$$\tilde{n}_l = \boldsymbol{w}_l^T \boldsymbol{n}_l, \tag{3.5}$$

so that the total vector $\tilde{\boldsymbol{n}}$ has distribution

$$\tilde{\boldsymbol{n}} \sim \mathcal{CN}\left(\boldsymbol{0}, N_0 \boldsymbol{I}\right). \tag{3.6}$$

Equation (3.6) holds true because the samples of $\boldsymbol{n}_k$ are independent among each other. Furthermore, the normalization considered in $\boldsymbol{W}$ will assure that the noise component obtained in each time slot is not amplified.

The estimation of the AoA will be done using Maximum Likelihood Estimation (MLE) since this estimation is asymptotically optimum [19]. This estimation maximizes the likelihood function defined as the conditional PDF of $\boldsymbol{y}$ given the parameter ϑ

$$L(\vartheta) = p(\boldsymbol{y}; \vartheta). \tag{3.7}$$

Therefore, we can express the ML estimator as

$$\hat{\vartheta}_{\mathrm{ML}} = \arg\max_{\vartheta} \ p(\boldsymbol{y}; \vartheta). \tag{3.8}$$

where $p(\boldsymbol{y}; \vartheta)$ is given by

$$p(\boldsymbol{y}; \vartheta) = \frac{1}{\sqrt{(\pi N_0)^L}} \exp\left(-\frac{\left\| \boldsymbol{y} - \boldsymbol{W}^T \boldsymbol{a}(\theta) \right\|^2}{N_0} \right). \tag{3.9}$$

Since this estimator can be shown to be too difficult for analytic computation, we will use a numerical algorithm to get a good approximate solution instead. The algorithm will calculate $L(\vartheta)$ over a sweep of ϑ values, select the value of ϑ that gives the maximum $L(\vartheta)$, and refine the result by doing a new sweep around the ϑ obtained before and getting the new ϑ that gives the maximum $L(\vartheta)$.

Now that we have defined our estimation problem, it is our main interest to see how the differently optimized codebooks obtained in the previous chapter perform in this problem. To do so, we will take the matrix $\boldsymbol{W}$ in (3.3) as one of the optimized codebooks from Chapter 2.

3.2 Estimation Performance of the Optimized Codebooks

Taking the optimized codebooks obtained from the previous chapter, we would like to see what influence the performance metrics being optimized for, as well as the optimization method, have on the performance for the AoA estimation. To do so, we perform simulations where we estimate the AoA using the different optimized codebooks. We would like to answer the question: "In order to obtain high precision in the AoA estimation, should the codebook be optimized for L_{avg} or $L_{\max}$, and using pure phase optimization of steering optimization?".

We evaluate the performance of each phase codebook as the MSE (Mean Squared Error) committed in the estimation using that codebook with respect to the true value

$$\text{MSE}(\vartheta) = \mathbb{E}\{(\hat{\vartheta} - \vartheta)^2\}. \tag{3.10}$$

Since we are interested in the whole range Ω_{140° we have to average ϑ over this range assuming that the AoA is uniformly distributed in this range. So this gives us

$$\begin{aligned} \text{MSE}_{\text{avg}} &= \frac{1}{S_\Omega} \int_\Omega \text{MSE}(\vartheta) \mathrm{d}\vartheta \\ &= \frac{1}{140} \int_{-70}^{70} \text{MSE}(\vartheta) \mathrm{d}\vartheta. \end{aligned} \tag{3.11}$$

Thus, we run simulations to analyze the performance of each of the optimized codebooks in terms of MSE_{avg} as defined in (3.11).

3.2.1 Simulation results

In Figure 3.1 we can see the MSE results for the differently optimized codebooks. The results are apparently not as positive as we would have expected beforehand.

As we can see, for some SNR values the steering optimization performs better than the pure phase optimization. In the region below -10dB the best codebook is the one associated to the steering optimization for $L_{\max}$, in the region between -10dB and -2dB the pure phase optimization for L_{avg} is best, while above -2dB the best one is the codebook associated to the steering optimization for L_{avg}, although they all converge to $\text{MSE}_{\text{avg}} = 0$ if the SNR is sufficiently high.

These results make sense since we are considering that the signal $\boldsymbol{y}(\vartheta)$ is being *detected* properly in all cases. This means that if the received signal is coming from an angle that corresponds to a minimum in the total array gain of one codebook we could still estimate its AoA, since if $\boldsymbol{y}(\vartheta)$ is almost 0 we would say that the received signal is coming from one of the directions where we have a minimum in $G_{\text{T}}(\vartheta)$. However, in a real scenario this would not be possible since the first step would be to know if we are actually receiving any signal and then to estimate the AoA associated to that signal. In other words, if we do not receive any signal we are not able to to detect any AoA; we would rather say that the signal is absent.

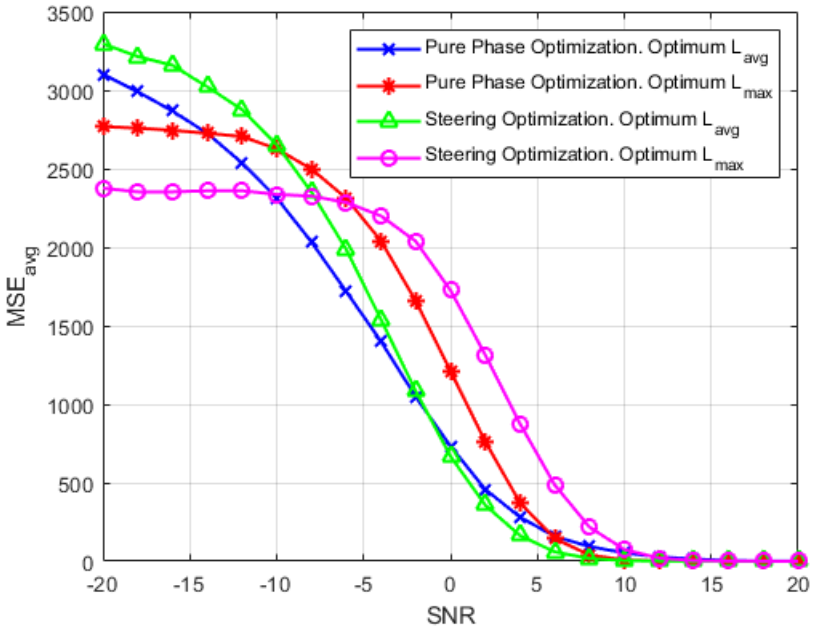

Figure 3.1: MSE of the estimator for the different optimized codebooks.

3.3 Detection Performance of the Optimized Codebooks

After taking a look at the simulation results for the AoA estimation performance of the codebooks in the previous section, and noticing that these results are assuming perfect detection, we find it interesting to take a look at how these codebooks actually perform in terms of detection performance. This means that we are interested now in knowing under which conditions would the different codebooks be able to detect an incoming signal in any of the possible AoAs uniformly distributed in the space defined. We use the same system model as we defined at the beginning of the chapter, but now we will focus on detecting if the received signal after the phase shift modules, $\boldsymbol{y}$ (in this case the dependence on ϑ doesn't concern us since we are not interested in estimating it), contains the signal $\boldsymbol{W}^T\boldsymbol{a}(\vartheta)$ or if it is just noise, thus we have two possible hypothesis

$$\mathcal{H}_0 : \boldsymbol{y} = \tilde{\boldsymbol{n}} \tag{3.12a}$$

$$\mathcal{H}_1 : \boldsymbol{y} = \boldsymbol{W}^T\boldsymbol{a}(\vartheta) + \tilde{\boldsymbol{n}}, \tag{3.12b}$$

where $\mathcal{H}_0$ corresponds to assuming that there is no received signal while $\mathcal{H}_1$ assumes that there is a received signal at a certain angle. Note that $\mathcal{H}_1$ is a composite hypothesis [20] where ϑ can take any value in the space defined, since $\vartheta \sim \mathcal{U}(-70, 70)$.

To compare the performance of the different optimized codebooks we obtain the ROC curves associated to each of them. These curves relate P_{D} and P_{FA}, defined respectively as the probability of detecting the signal when it is present, and the probability of detecting a signal when it is not present (false alarm).

According to the Neyman-Pearson lemma [20], to maximize P_{D} for a given P_{FA}, $\mathcal{H}_1$ should be selected if

$$L(\boldsymbol{y}) = \frac{p(\boldsymbol{y}; \mathcal{H}_1)}{p(\boldsymbol{y}; \mathcal{H}_0)} > \gamma, \tag{3.13}$$

where γ is related to the given P_{FA} through

$$P_{\mathrm{FA}} = \int_{L(\boldsymbol{y})>\gamma} p(\boldsymbol{y}; \mathcal{H}_0)\mathrm{d}\boldsymbol{y} \tag{3.14}$$

while P_{D} is obtained by

$$P_{\mathrm{D}} = \int_{L(\boldsymbol{y})>\gamma} p(\boldsymbol{y}; \mathcal{H}_1)\mathrm{d}\boldsymbol{y}. \tag{3.15}$$

The PDF under $\mathcal{H}_0$ is given directly by

$$p(\boldsymbol{y}; \mathcal{H}_0) = \frac{1}{(\pi N_0)^L} \exp\left(-\frac{\|\boldsymbol{y}\|^2}{N_0}\right) \tag{3.16}$$

$$\|\boldsymbol{y}\|^2 = \sum_{i=1}^{L} |y_i|^2 \tag{3.17}$$

with $L = 2$ in this case, corresponding to the number of codewords in the codebook, and thus the length of vector $\boldsymbol{y}$.

For the PDF under $\mathcal{H}_1$, since it is a composite hypothesis with a random variable we need to take a different approach. We have two possibilities, the Bayesian approach and the GLRT (Generalized Likelihood Ratio Test) approach. The Bayesian approach consists in defining $p(\boldsymbol{y}; \mathcal{H}_1)$ as

$$\begin{aligned} p(\boldsymbol{y}; \mathcal{H}_1) &= \int_{\Omega} p(\boldsymbol{y}|\vartheta; \mathcal{H}_1) p(\vartheta) \mathrm{d}\vartheta \\ &= \frac{1}{140} \int_{-70}^{70} p(\boldsymbol{y}|\vartheta; \mathcal{H}_1) \mathrm{d}\vartheta, \end{aligned} \tag{3.18}$$

where $p(\boldsymbol{y}|\vartheta; \mathcal{H}_1)$ equals

$$p(\boldsymbol{y}|\vartheta; \mathcal{H}_1) = \frac{1}{(\pi N_0)^L} \exp\left(-\frac{\left\| \boldsymbol{y} - \boldsymbol{W}^T \boldsymbol{a}(\theta) \right\|^2}{N_0} \right). \tag{3.19}$$

The GLRT (Generalized Likelihood Ratio Test) approach consists of first assuming $\mathcal{H}_1$ and obtaining $\hat{\vartheta}$ as the MLE, and then defining $p(\boldsymbol{y}; \mathcal{H}_1)$ as

$$p(\boldsymbol{y}; \mathcal{H}_1) = p(\boldsymbol{y}|\hat{\vartheta}; \mathcal{H}_1). \tag{3.20}$$

We will be using the Bayesian approach since it offers a better performance (although we will also check the GLRT to compare them).

With these considerations, we run simulations to obtain the ROC curves associated to the different codebooks. To do so, we compute $p(\boldsymbol{y}; \mathcal{H}_1)$ and $p(\boldsymbol{y}; \mathcal{H}_0)$ for a number of realizations of $\boldsymbol{y}$, considering that both $\tilde{\boldsymbol{n}}$ and ϑ are random, and get the P_{FA} and P_{D} using (3.13) for a sweep of γ values.

3.3.1 Simulation results

In Figures 3.2-3.6 we show the ROC curves resulting from the simulations for different SNR values. We can see that in general the curves associated to codebooks using pure phase optimization perform better, and more specifically the one optimizing $L_{\max}$ is generally the best. However, if we take a close look at the curves for low SNR, specially in Figure 3.2, we notice that for low P_{FA} values (in general we would like a low P_{FA} value so that we don't waste energy on trying to decode noise) the curves cross each other and the steering optimization for L_{avg} performs better than the rest in some cases. This fact is eliminated as SNR goes above 0dB, and we see that the performance of pure phase optimization gets a clearer gain in detection performance as SNR grows until the curves begin to saturate at SNR over 10dB. This saturation may happen when the SNR is sufficiently high so that the received power is high enough even at the directions where the total array gain reaches the value $L_{\max}$.

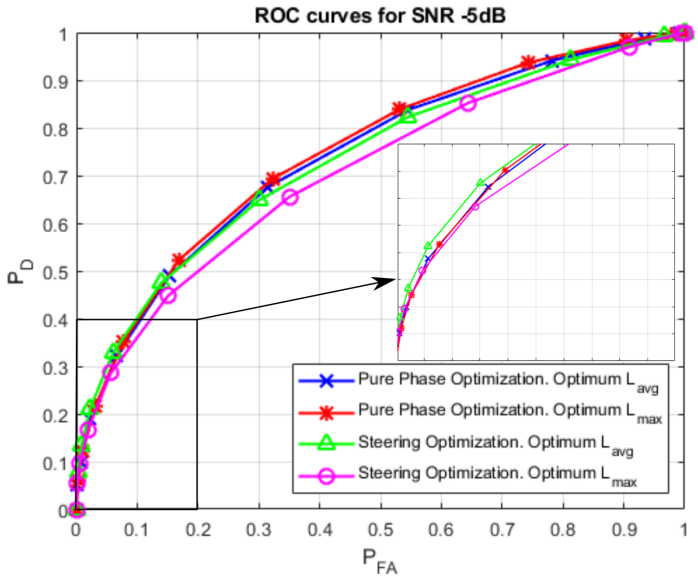

Figure 3.2: ROC curves for the optimized codebooks at SNR $= -5$dB.

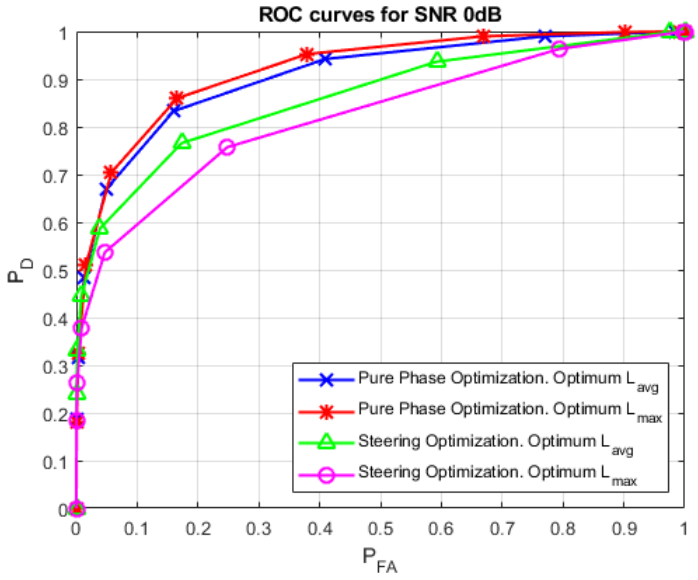

Figure 3.3: ROC curves for the optimized codebooks at SNR $= 0$dB.

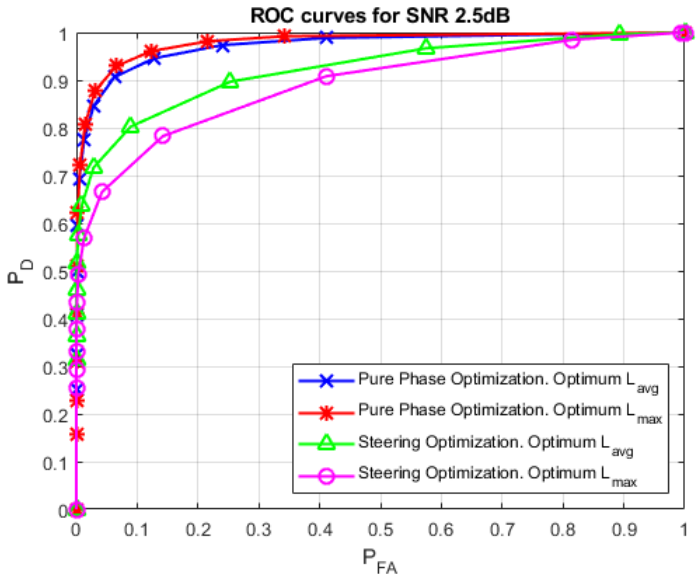

Figure 3.4: ROC curves for the optimized codebooks at SNR = 2.5dB.

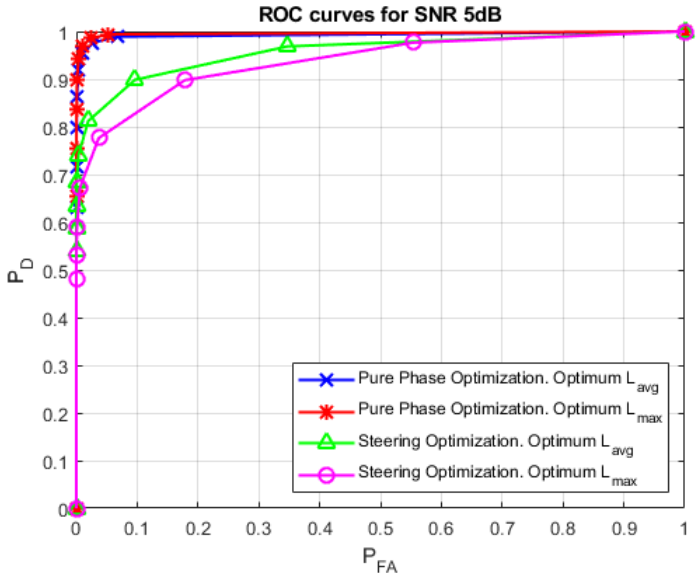

Figure 3.5: ROC curves for the optimized codebooks at SNR = 5dB.

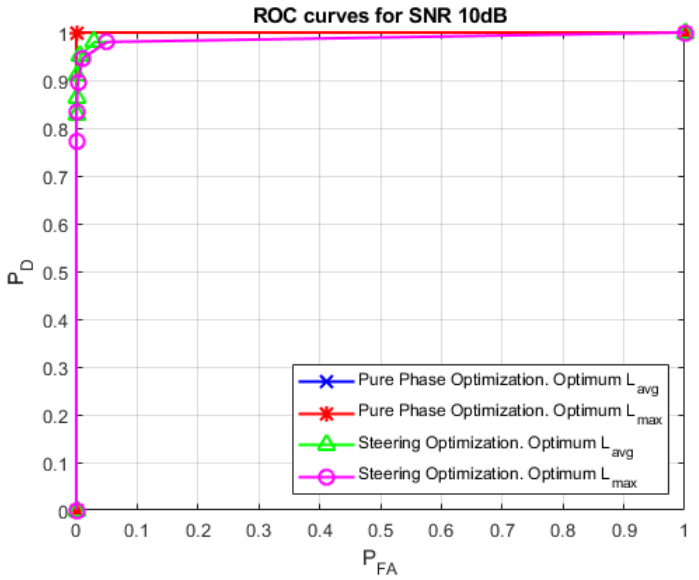

Figure 3.6: ROC curves for the optimized codebooks at SNR = 10dB.

3.4 Concluding Remarks

In this chapter we have analyzed the AoA estimation using the optimized phase codebooks obtained in the previous chapter. We have seen that the pure phase optimized codebooks don't pose a clear improvement in terms of MSE in the AoA estimation. Nevertheless, this could be explained by the fact that for the MSE calculations we assume perfect detection, and not all the codebooks have the same detection performance.

So as to check the detection performance we have simulated the ROC curves for the different codebooks. We have observed that in general the pure phase optimized codebooks, specially the one optimizing $L_{\max}$, offer a better detection performance. We can expect therefore that the most important metric for this detection performance is $L_{\max}$, which it is the one that the pure phase optimization can improve the most over the steering optimization if we look at Table 2.1. Now we would like to find an explanation to this improvement in detection performance, but the scenario looks too complex to analyze it theoretically. Therefore, in the next chapter we will take a simplified scenario related to the original one to be able to analyze it theoretically and get some understanding about how this detection performance is affected by the metrics L_{avg} and $L_{\max}$.

Chapter 4
Detection Performance in a Simplified Scenario

In this chapter a simplified scenario will be presented and analyzed to get some insights regarding the detection performance of our optimized codebooks. We would like to understand why the pure phase optimized codebooks, and above all the one optimizing $L_{\max}$, perform better than the rest. As we could see in the previous chapter, $L_{\max}$ is the metric that should be reduced to get a better detection performance, so we will try to define a scenario which allows to see this relationship.

4.1 Scenario Definition

If we look at the original scenario from Chapter 3 we can see that we are just receiving a vector containing complex exponentials associated to the AoA plus some noise, multiplying it by a certain codebook and trying to estimate the AoA from the resulting signal. This is equivalent in some way to introducing a pure tone plus some noise to a specific filter or channel with a known response in frequency, and determining the frequency of the signal.

It is clear that a pure tone in the time domain is just a complex exponential associated to the frequency of the tone and filtering it would mean to multiply it in frequency by a certain value, although for pure tones this multiplication in the frequency domain can be translated to a multiplication in the time domain since the bandwidth is close to 0. If we focus on the frequency domain, without loss of generality, we can get a simplified scenario which will give us understanding of our original problem. Furthermore, we can define a filter such that it has just two values throughout its bandwidth. The first value, A, will be associated to the metric $L_{\max}$ of the original scenario, and the second value, B, will be associated to the MRC gain , with $A < B$.

So the scenario can be seen as a transmitted signal $\boldsymbol{x}$ that takes the value 1 at a random position p while having the rest of the positions equal to 0. The total length of $\boldsymbol{x}$ is P so that $p \sim \mathcal{U}(0, P-1)$. This signal goes through a channel which takes the value A for $p \leq C$ and B for $p > C$ and adds AWGN of variance $N_0/2$. Therefore, the received signal is

$$\boldsymbol{y} = \boldsymbol{D}\boldsymbol{x} + \boldsymbol{n}, \tag{4.1}$$

where $\boldsymbol{n}$ is the noise signal $\boldsymbol{n} \sim \mathcal{N}(0, N_0/2)$, and $\boldsymbol{D} = \text{diag}(\lambda_1, \lambda_2, ..., \lambda_P)$ is the diagonal matrix representing the channel or filter response

$$\lambda_i = \begin{cases} A & \text{if} \quad i \leq C \\ B & \text{if} \quad i > C. \end{cases} \tag{4.2}$$

Our interest is to analyze the detection performance in the scenario with respect to the parameters A, B and C that define the channel. We can therefore define two possible hypothesis $\mathcal{H}_0$ and $\mathcal{H}_1$, where $\mathcal{H}_0$ corresponds to the case where the transmitted signal $\boldsymbol{x}$ is not present ($\boldsymbol{x} = \boldsymbol{0}$) and $\mathcal{H}_1$ corresponds to the case where it is present

$$\mathcal{H}_0 : \boldsymbol{y} = \boldsymbol{n} \tag{4.3a}$$

$$\mathcal{H}_1 : \boldsymbol{y} = \boldsymbol{D}\boldsymbol{x} + \boldsymbol{n}. \tag{4.3b}$$

Note that these equations are similar to (3.12).

So it can be clearly seen that under $\mathcal{H}_0$, $\boldsymbol{y} \sim \mathcal{N}(0, N_0/2)$ while under $\mathcal{H}_1$, $\boldsymbol{y} \sim \mathcal{N}(\boldsymbol{D}\boldsymbol{x}, N_0/2\boldsymbol{I})$. Since $\boldsymbol{x}$ has an unknown random parameter p we will have to take a composite hypothesis testing approach.

4.2 Detection Probability Characterization

4.2.1 Calculations

We can take again the Neyman-Pearson lemma (3.13) to maximize P_{D} given P_{FA}. A reader not interested in the detailed derivation of P_{D} can proceed directly to Equation (4.24), where the result is stated. Under $\mathcal{H}_0$ the PDF is perfectly known and gives

$$p(\boldsymbol{y}; \mathcal{H}_0) = \frac{1}{\sqrt{(\pi N_0)^P}} \exp\left(-\frac{\|\boldsymbol{y}\|^2}{N_0}\right) \tag{4.4}$$

$$\|\boldsymbol{y}\|^2 = \sum_{i=1}^{P} |y_i|^2. \tag{4.5}$$

However, as we mentioned before $\mathcal{H}_1$ has a PDF containing a random parameter p. This means that we need a composite hypothesis testing approach for defining $p(\boldsymbol{y}; \mathcal{H}_1)$. Due to its good performance we will use again a Bayesian approach where in this case

$$p(\boldsymbol{y}; \mathcal{H}_1) = \int p(\boldsymbol{y}|p; \mathcal{H}_1) p(p) \mathrm{d}p. \tag{4.6}$$

In our case p is a discrete uniformly distributed random variable, so we can express this integral as

$$p(\boldsymbol{y}; \mathcal{H}_1) = \frac{1}{P} \sum_{i=1}^{P} p(\boldsymbol{y}|p; \mathcal{H}_1). \tag{4.7}$$

The PDF $p(\boldsymbol{y}|p;\mathcal{H}_1)$ corresponds to

$$\begin{aligned} p(\boldsymbol{y}|p;\mathcal{H}_1) &= \frac{1}{\sqrt{(\pi N_0)^P}} \exp\left(-\frac{(y_p-\lambda_p)^2}{N_0}\right) \exp\left(-\frac{\sum_{i\neq p} y_i^2}{N_0}\right) \\ &= \begin{cases} \frac{1}{\sqrt{(\pi N_0)^P}} \exp\left(-\frac{(y_p-A)^2}{N_0}\right) \exp\left(-\frac{\sum_{i\neq p} y_i^2}{N_0}\right) & \text{if} \quad p \leq C \\ \frac{1}{\sqrt{(\pi N_0)^P}} \exp\left(-\frac{(y_p-B)^2}{N_0}\right) \exp\left(-\frac{\sum_{i\neq p} y_i^2}{N_0}\right) & \text{if} \quad p > C. \end{cases} \end{aligned} \tag{4.8}$$

If we simplify the expression we get

$$\begin{aligned} p(\boldsymbol{y}|p;\mathcal{H}_1) &= \frac{1}{\sqrt{(\pi N_0)^P}} \exp\left(-\frac{(y_p-\lambda_p)^2 - y_p^2}{N_0}\right) \exp\left(-\frac{\sum_{i=0}^{P-1} {y_i}^2}{N_0}\right) \\ &= \frac{1}{\sqrt{(\pi N_0)^P}} \exp\left(\frac{2y_p\lambda_p - \lambda_p^2}{N_0}\right) \exp\left(-\frac{\|\boldsymbol{y}\|^2}{N_0}\right). \end{aligned} \tag{4.9}$$

Taking the Bayesian approach we get

$$\begin{aligned} p(\boldsymbol{y};\mathcal{H}_1) &= \frac{1}{P}\sum_{p=1}^{P} \frac{1}{\sqrt{(\pi N_0)^P}} \exp\left(\frac{2y_p\lambda_p - \lambda_p^2}{N_0}\right) \exp\left(-\frac{\|\boldsymbol{y}\|^2}{N_0}\right) \\ &= \frac{\exp\left(-\frac{\|\boldsymbol{y}\|^2}{N_0}\right)}{P\sqrt{(\pi N_0)^P}} \sum_{p=1}^{P} \exp\left(\frac{2y_p\lambda_p - \lambda_p^2}{N_0}\right) \\ &= \frac{\exp\left(-\frac{\|\boldsymbol{y}\|^2}{N_0}\right)}{P\sqrt{(\pi N_0)^P}} \left[\sum_{i=1}^{C} \exp\left(\frac{2y_iA - A^2}{N_0}\right) \right. \\ &\quad \left. + \sum_{j=C+1}^{P} \exp\left(\frac{2y_jB - B^2}{N_0}\right)\right]. \end{aligned} \tag{4.10}$$

This gives us a likelihood ratio of

$$\begin{aligned} L(\boldsymbol{y}) &= \frac{p(\boldsymbol{y};\mathcal{H}_1)}{p(\boldsymbol{y};\mathcal{H}_0)} \\ &= \frac{1}{P}\sum_{i=1}^{C} \exp\left(\frac{2y_iA - A^2}{N_0}\right) + \sum_{j=C+1}^{P} \exp\left(\frac{2y_jB - B^2}{N_0}\right) \\ &= \frac{1}{P}\sum_{i=1}^{P} \exp\left(\frac{2y_i\lambda_i - \lambda_i^2}{N_0}\right). \end{aligned} \tag{4.11}$$

From (4.3) it can be derived that under $\mathcal{H}_0$, $y_i \sim \mathcal{N}(0, N_0/2)\ \forall i \in [0,\, P-1]$. On the other hand, under $\mathcal{H}_1$, these random variables depend on the position p of the 1 in $\boldsymbol{x}$. This means that, under $\mathcal{H}_1$,

$$y_i \sim \begin{cases} \mathcal{N}(A,\, N_0/2) & \text{if} \quad i = p \quad \text{and} \quad p \leq C \\ \mathcal{N}(B,\, N_0/2) & \text{if} \quad i = p \quad \text{and} \quad p > C \\ \mathcal{N}(0,\, N_0/2) & \text{if} \quad i \neq p. \end{cases} \tag{4.12}$$

The term inside the exponentials in (4.11) is also a normal random variable since it is formed from a multiplication and a sum with a constant value. It can be easily derived that under $\mathcal{H}_1$

$$2y_i\lambda_i - \lambda_i^2 \sim \begin{cases} \mathcal{N}\left(\frac{A^2}{N_0},\, \frac{2A^2}{N_0}\right) & \text{if} \quad i = p \quad \text{and} \quad p \leq C \\ \mathcal{N}\left(\frac{B^2}{N_0},\, \frac{2B^2}{N_0}\right) & \text{if} \quad i = p \quad \text{and} \quad p > C \\ \mathcal{N}\left(-\frac{A^2}{N_0},\, \frac{2A^2}{N_0}\right) & \text{if} \quad i \neq p \quad \text{and} \quad i \leq C \\ \mathcal{N}\left(-\frac{B^2}{N_0},\, \frac{2B^2}{N_0}\right) & \text{if} \quad i \neq p \quad \text{and} \quad i > C. \end{cases} \tag{4.13}$$

Under $\mathcal{H}_0$ the same random variable would be distributed as in the case where $i \neq p$ under $\mathcal{H}_1$. By definition, the exponential of a normal random gives a log-normal random variable. Our likelihood function $L(\boldsymbol{y})$ is therefore a sum of log-normal random variables. Furthermore, the mean and variance of each of these variables may not be the same as we can predict from (4.13). All this makes $L(\boldsymbol{y})$ to be distributed in an apparently unknown way. However, as discussed in [21], we could approximate this distribution as a log-normal distribution with mean and variance being the sum of the means and variances respectively of each of the log-normal variables being summed.

If we have a normally distributed random variable with mean μ and variance σ^2, the log-normal random variable resulting from taking the exponential of this normal random variable will have mean $\mu_{\log}$ and variance $\sigma^2_{\log}$

$$\mu_{\log} = \exp\left(\mu + \frac{\sigma^2}{2}\right) \tag{4.14a}$$

$$\sigma^2_{\log} = (\exp(\sigma^2) - 1)\exp(2\mu + \sigma^2). \tag{4.14b}$$

Therefore, we can get the distribution for the exponentials under $\mathcal{H}_1$ as

$$\exp(2y_i\lambda_i - \lambda_i^2) \sim \begin{cases} \mathcal{LN}\left[\exp\left(\frac{2A^2}{N_0}\right), \left(\exp\left(\frac{2A^2}{N_0}\right)-1\right)\exp\left(\frac{4A^2}{N_0}\right)\right] & \text{if } i=p, \text{ and } p \leq C \\ \mathcal{LN}\left[\exp\left(\frac{2B^2}{N_0}\right), \left(\exp\left(\frac{2B^2}{N_0}\right)-1\right)\exp\left(\frac{4B^2}{N_0}\right)\right] & \text{if } i=p, \text{ and } p > C \\ \mathcal{LN}\left(1, \exp\left(\frac{2A^2}{N_0}\right)-1\right) & \text{if } i \neq p, \text{ and } p \leq C \\ \mathcal{LN}\left(1, \exp\left(\frac{2B^2}{N_0}\right)-1\right) & \text{if } i \neq p, \text{ and } p > C. \end{cases} \tag{4.15}$$

Again, under $\mathcal{H}_0$ the distribution would correspond to the case where $i \neq p$. The mean and variance of the likelihood function under $\mathcal{H}_0$ will then be

$$\mathbb{E}\{L(\boldsymbol{y};\mathcal{H}_0)\} = \frac{1}{P}(C+P-C) = 1 \tag{4.16a}$$

$$\begin{aligned}\mathrm{Var}\{L(\boldsymbol{y};\mathcal{H}_0)\} = \frac{1}{P^2}\Bigg[&C\left(\exp\left(\frac{2A^2}{N_0}\right)-1\right) \\ &+(P-C)\left(\exp\left(\frac{2B^2}{N_0}\right)-1\right)\Bigg].\end{aligned} \tag{4.16b}$$

Under $\mathcal{H}_1$ we have the case that $p \leq C$ and the case that $p > C$

$$\begin{aligned}\mathbb{E}\{L(\boldsymbol{y}|p \leq C;\mathcal{H}_1)\} &= \frac{1}{P}\left(C-1+P-C+\exp\left(\frac{2A^2}{N_0}\right)\right) \\ &= \frac{1}{P}\left(P+\exp\left(\frac{2A^2}{N_0}\right)-1\right)\end{aligned} \tag{4.17a}$$

$$\begin{aligned}\mathrm{Var}\{L(\boldsymbol{y}|p \leq C;\mathcal{H}_1)\} = \frac{1}{P^2}\Bigg[&(C-1)\left(\exp\left(\frac{2A^2}{N_0}\right)-1\right) \\ &+(P-C)\left(\exp\left(\frac{2B^2}{N_0}\right)-1\right) \\ &+\left(\exp\left(\frac{2A^2}{N_0}\right)-1\right)\exp\left(\frac{4A^2}{N_0}\right)\Bigg].\end{aligned} \tag{4.17b}$$

$$\mathbb{E}\{L(\boldsymbol{y}|p \leq C; \mathcal{H}_1)\} = \frac{1}{P}\left(C - 1 + P - C + \exp\left(\frac{2B^2}{N_0}\right)\right)$$
$$= \frac{1}{P}\left(P + \exp\left(\frac{2B^2}{N_0}\right) - 1\right) \tag{4.18a}$$
$$\mathrm{Var}\{L(\boldsymbol{y}|p \leq C; \mathcal{H}_1)\} = \frac{1}{P^2}\left[C\left(\exp\left(\frac{2A^2}{N_0}\right) - 1\right)\right.$$
$$+ (P - C - 1)\left(\exp\left(\frac{2B^2}{N_0}\right) - 1\right) \tag{4.18b}$$
$$\left. + \left(\exp\left(\frac{2B^2}{N_0}\right) - 1\right)\exp\left(\frac{4B^2}{N_0}\right)\right].$$

Now that we have characterized $L(\boldsymbol{y})$ as a log-normal distribution, with a mean and variance for the different cases, we can take the logarithm of it. This means obtaining the log-likelihood function, $\ln(L(\boldsymbol{y}))$, which should be distributed approximately as a normal random variable. In order to obtain the mean and variance of $\ln(L(\boldsymbol{y}))$ we can use the results in (4.16), (4.17) and (4.18), and derive using (4.14)

$$\mu = \ln(\mu_{\log}) - \frac{1}{2}\ln\left(\frac{\sigma^2_{\log}}{\mu^2_{\log}} + 1\right) \tag{4.19a}$$
$$\sigma^2 = \ln\left(\frac{\sigma^2_{\log}}{\mu^2_{\log}} + 1\right). \tag{4.19b}$$

The final expressions are too long to write them down and analyze them, but they can be computed easily with the help of software tools.

Now we are able to characterize approximately the log-likelihood function by a normal distribution $\ln(L(\boldsymbol{y})) \sim \mathcal{N}(\mu, \sigma^2)$ with a fixed mean and variance for $\mathcal{H}_0$, $\mu_{\mathcal{H}_0}$ and $\sigma^2_{\mathcal{H}_0}$. Under $\mathcal{H}_1$, however, the log-likelihood function can take one of two sets of possible means and variances:

$$\ln(L(\boldsymbol{y}|p \leq C; \mathcal{H}_1)) \sim \mathcal{N}(\mu_{\mathcal{H}_1\mathrm{A}}, \sigma^2_{\mathcal{H}_1\mathrm{A}}) \tag{4.20}$$

when the uniformly distributed random variable p takes values below C, and

$$\ln(L(\boldsymbol{y}|p > C; \mathcal{H}_1)) \sim \mathcal{N}(\mu_{\mathcal{H}_1\mathrm{B}}, \sigma^2_{\mathcal{H}_1\mathrm{B}}) \tag{4.21}$$

in the complementary case. In this case it poses no problem since p is uniformly distributed and we can just average the two distributions considering the length of the intervals where each of the distributions take place.

With all these derivations we consider again the Neyman-Pearson lemma (3.13) [20], where in this case we have taken the logarithm, but since it is a monotonic function it only affects to the fact that the variable γ is now a different one γ'. We get P_{FA} from (3.14)

$$\begin{aligned} P_{\text{FA}} &= \int_{\ln(L(\boldsymbol{y}))>\gamma'} p(\boldsymbol{y};\mathcal{H}_0)\mathrm{d}\boldsymbol{y} \\ &= \mathrm{Q}\left(\frac{\gamma'-\mu_{\mathcal{H}_0}}{\sqrt{\sigma^2_{\mathcal{H}_0}}}\right). \end{aligned} \tag{4.22}$$

From this result we can also get γ' as a function of P_{FA}

$$\gamma' = \sqrt{\sigma^2_{\mathcal{H}_0}}\mathrm{Q}^{-1}(P_{\text{FA}}) + \mu_{\mathcal{H}_0}. \tag{4.23}$$

P_{D} can be also computed as

$$\begin{aligned} P_{\text{D}} &= \int_{\ln(L(\boldsymbol{y}))>\gamma'} p(\boldsymbol{y};\mathcal{H}_1)\mathrm{d}\boldsymbol{y} \\ &= \frac{C}{P}\,\mathrm{Q}\left(\frac{\gamma'-\mu_{\mathcal{H}_1\text{A}}}{\sqrt{\sigma^2_{\mathcal{H}_1\text{A}}}}\right)\frac{P-C}{P}\,\mathrm{Q}\left(\frac{\gamma'-\mu_{\mathcal{H}_1\text{B}}}{\sqrt{\sigma^2_{\mathcal{H}_1\text{B}}}}\right) \\ &= \alpha\,\mathrm{Q}\left(\frac{\sqrt{\sigma^2_{\mathcal{H}_0}}\mathrm{Q}^{-1}(P_{\text{FA}})+\mu_{\mathcal{H}_0}-\mu_{\mathcal{H}_1\text{A}}}{\sqrt{\sigma^2_{\mathcal{H}_1\text{A}}}}\right) \\ &\quad +(1-\alpha)\,\mathrm{Q}\left(\frac{\sqrt{\sigma^2_{\mathcal{H}_0}}\mathrm{Q}^{-1}(P_{\text{FA}})+\mu_{\mathcal{H}_0}-\mu_{\mathcal{H}_1\text{B}}}{\sqrt{\sigma^2_{\mathcal{H}_1\text{B}}}}\right), \end{aligned} \tag{4.24}$$

where we have defined $\alpha = C/P$.

4.2.2 Validation of the results

For the validation of (4.24), where we have used approximations that may not be tight in all cases, we will run simulations of the scenario defined and compare the results with those obtained using the formula we have obtained. For normalization purposes, we set the total power of the channel to 1, i.e.,

$$A^2\alpha P + B^2(1-\alpha)P = 1. \tag{4.25}$$

We also define the product $N_0 \times P$ instead of just N_0 so that the SNR is maintained.

In Figures 4.1-4.10 we have the ROC curves comparing the simulated results and the calculated ones. We can see that in general the approximations leading

to (4.24) are fairly accurate. However, as SNR decreases, which can be related to $\frac{1}{P \times N_0}$, we can see that the approximation gets worse performance. This effect is higher if we lower the α value, where the limiting SNR gets lower as can be seen from Figures 4.8 or 4.6. Therefore, the most limiting case in terms of SNR for the approximation to withhold is the case for $\alpha = 0$, where we can note that in this case the A value doesn't affect at all. Thus, we can see that it is equivalent in this sense to use a low α to using an A value close to the B value (it's the same setting $A = B$ and setting $\alpha = 0$) as can be seen from Figure 4.4. Another thing we have noticed from Figures 4.9 and 4.10 regarding our approximation is that, if we increase P with respect to the SNR, the formula is less accurate.

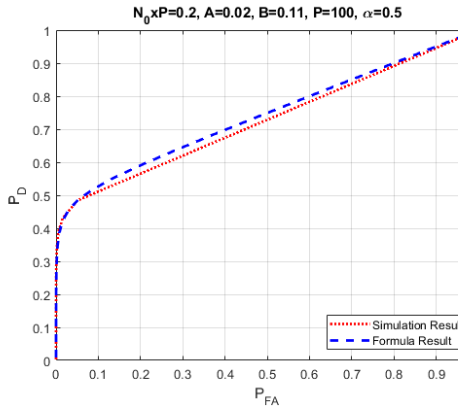

Figure 4.1: Simulated and calculated ROC curves for $N_0 \times P = 0.2$, $A = 0.02$, $B = 0.11$, $P = 100$ and $\alpha = 0.5$.

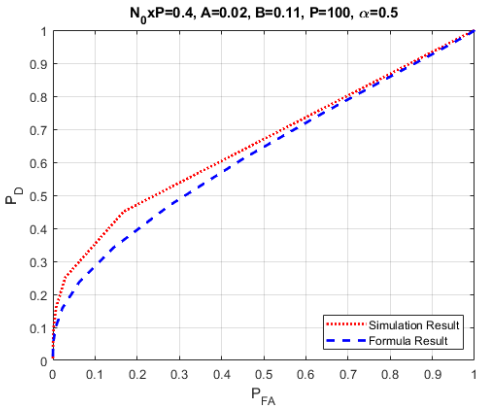

Figure 4.2: Simulated and calculated ROC curves for $N_0 \times P = 0.4$, $A = 0.02$, $B = 0.11$, $P = 100$ and $\alpha = 0.5$.

4.3 Simplification and Approximation

As it has been mentioned before, the final expressions for the statistics of the log-likelihood function are far too long and difficult to analyze. In order to make them more tractable, we are going to simplify the scenario and invoke approximations until we get a closed form formula easy enough to gain some understanding from.

4.3.1 Assumptions

So as to be able to simplify our results and to be able to apply approximations we have to make assumptions first. We consider from now on only the case in which the variable A, corresponding to the first value of the channel, is either 0 or equal to B, corresponding to the second value of the channel. Nonetheless, this second case is the same as to say that the value α defined in (4.24) is set to 0 and A is not considered at all.

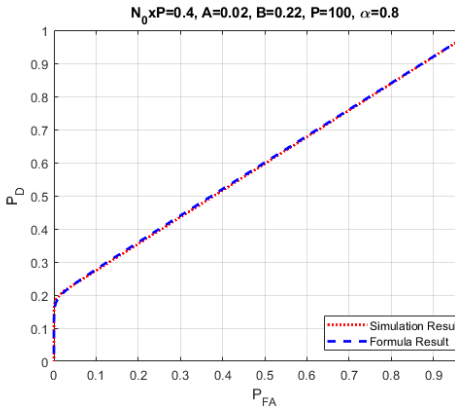

Figure 4.3: Simulated and calculated ROC curves for $N_0 \times P = 0.4$, $A = 0.02$, $B = 0.22$, $P = 100$ and $\alpha = 0.8$.

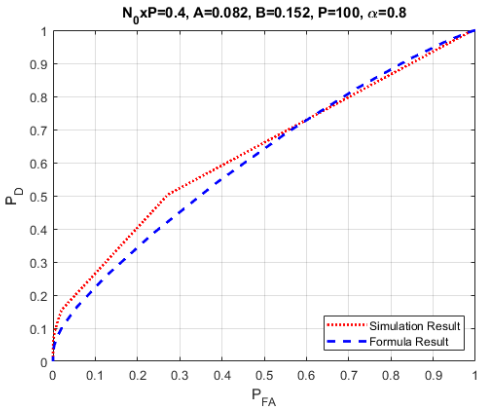

Figure 4.4: Simulated and calculated ROC curves for $N_0 \times P = 0.4$, $A = 0.02$, $B = 0.22$, $P = 100$ and $\alpha = 0.8$.

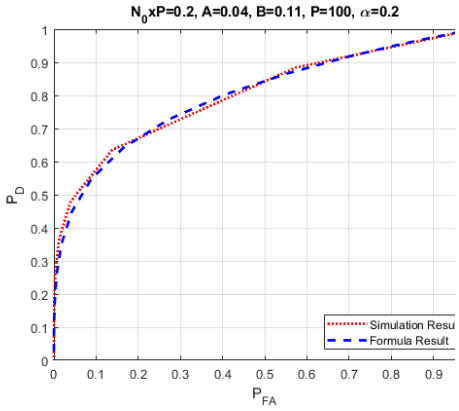

Figure 4.5: Simulated and calculated ROC curves for $N_0 \times P = 0.2$, $A = 0.04$, $B = 0.11$, $P = 100$ and $\alpha = 0.2$.

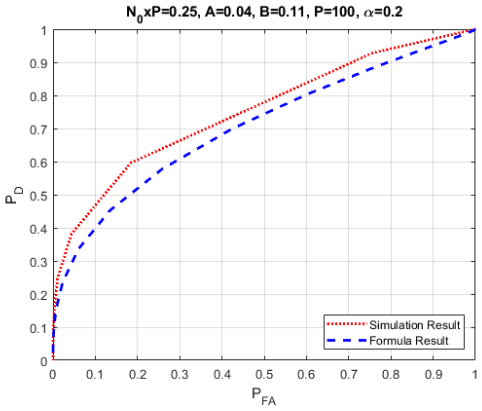

Figure 4.6: Simulated and calculated ROC curves for $N_0 \times P = 0.25$, $A = 0.04$, $B = 0.11$, $P = 100$ and $\alpha = 0.2$.

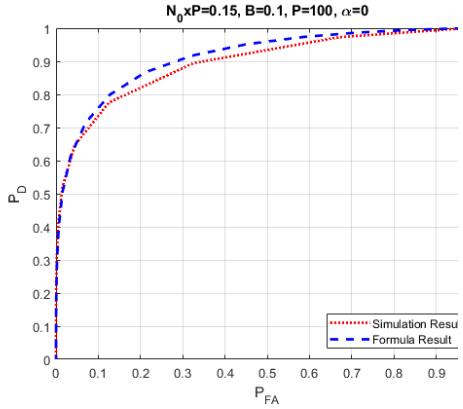

Figure 4.7: Simulated and calculated ROC curves for $N_0 \times P = 0.15$, $B = 0.1$, $P = 100$ and $\alpha = 0$.

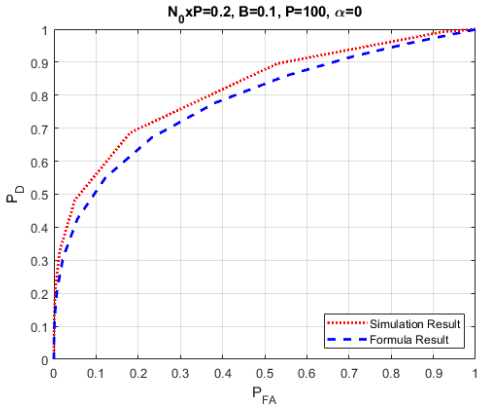

Figure 4.8: Simulated and calculated ROC curves for $N_0 \times P = 0.2$, $B = 0.1$, $P = 100$ and $\alpha = 0$.

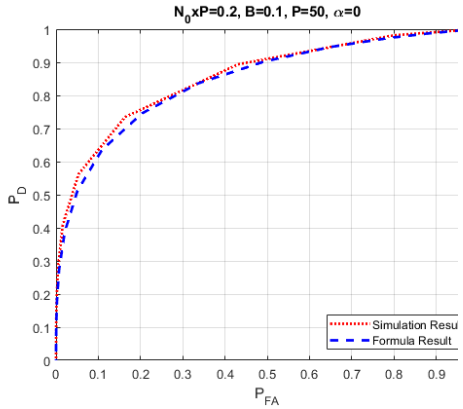

Figure 4.9: Simulated and calculated ROC curves for $N_0 \times P = 0.15$, $B = 0.1$, $P = 50$ and $\alpha = 0$.

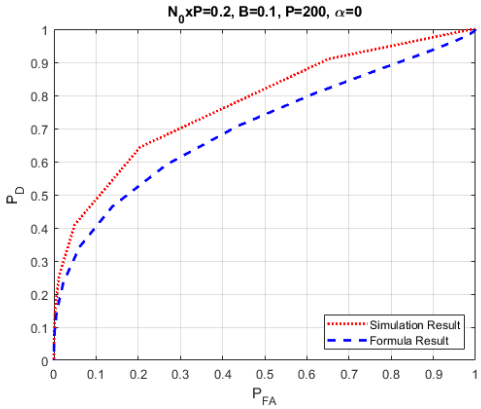

Figure 4.10: Simulated and calculated ROC curves for $N_0 \times P = 0.15$, $B = 0.1$, $P = 200$ and $\alpha = 0$.

The main goal of this model now is to compare the performance for different values of α. To do so we need to normalize then the value B so that the total power of the channel is kept constant. A good normalization is to set the total power of the channel to be 1

$$\|\boldsymbol{D}\|_F^2 = \text{trace}(\boldsymbol{D}^H\boldsymbol{D}) = (P-C)B^2 = P(1-\alpha)B^2 \tag{4.26}$$

Thus, this can be done just by setting

$$B = \frac{1}{\sqrt{P(1-\alpha)}} \tag{4.27}$$

Note that we are already considering that $A = 0$, and that $A = B$ is just done by setting $\alpha = 0$. However, with this normalization if we increase P, then B would get smaller and smaller, making the signal $\boldsymbol{y}$ to be almost noise. So as to remove this effect we will set

$$N_0 = \frac{N_{0\text{ref}}}{P} \tag{4.28}$$

$N_{0\text{ref}}$ being a reference noise spectral density. This way we can define our signal to noise ratio as

$$\text{SNR} = \frac{2(1-\alpha)B^2}{N_0} = \frac{2}{N_{0\text{ref}}} \tag{4.29}$$

which is constant over P. The factor 2 is just a scaling factor that comes in handy to simplify the expressions, but we would have to subtract $3dB$ to be able to compare with other real scenarios.

Another assumption that we will make is that we assume high SNR, more specifically

$$\exp\left(\frac{2B^2}{N_0}\right) \geq \exp(\text{SNR}) \gg 1 \tag{4.30}$$

and also, although this limits the approximation, especially for certain values of α, we assume

$$\frac{1}{P}\ \exp\left(\frac{2B^2}{N_0}\right) \gg 1. \tag{4.31}$$

Of course P has to be also big so that the previous approximations stand, but not as large as the exponential of $2B^2/N_0$.

4.3.2 Approximations

To simplify our expressions we will first take as starting point the expressions (4.16), (4.17) and (4.18). It can be easily seen that the expressions in (4.16) and (4.17) are the same for $A = 0$, so we will just have to simplify them once. A reader not interested in the detailed derivations can proceed directly to (4.42), where the formula (4.24) is presented after approximating.

Evaluating (4.17) at $A = 0$ we get

$$\begin{aligned}\mathbb{E}\{L(\boldsymbol{y}|p \leq C; \mathcal{H}_1)\} &= \mathbb{E}\{L(\boldsymbol{y}; \mathcal{H}_0)\} \\ &= \frac{1}{P}(P + 1 - 1) \\ &= 1 \qquad (4.32a) \\ \mathrm{Var}\{L(\boldsymbol{y}|p \leq C; \mathcal{H}_1)\} &= \mathrm{Var}\{L(\boldsymbol{y}; \mathcal{H}_0)\} \\ &= \frac{1}{P^2}\left[(P - C)\left(\exp\left(\frac{2B^2}{N_0}\right) - 1\right)\right] \\ &= \frac{1}{P}\left[(1 - \alpha)\left(\exp\left(\frac{2B^2}{N_0}\right) - 1\right)\right]. \qquad (4.32b)\end{aligned}$$

Then if we invoke the assumption (4.30) in (4.32b) we get

$$\mathrm{Var}\{L(\boldsymbol{y}; \mathcal{H}_0)\} \approx \frac{1}{P}\left[(1 - \alpha)\exp\left(\frac{2B^2}{N_0}\right)\right]. \qquad (4.33)$$

We next develop the expression under $\mathcal{H}_0$, although it is clear that it will be the same as $\mathcal{H}_1$ with $p \leq C$. Then, if we take (4.19) to get the mean and variance of the log-likelihood function we get

$$\mathbb{E}\{\ln(L(\boldsymbol{y}; \mathcal{H}_0))\} = -\frac{1}{2}\ln\left(\frac{1 - \alpha}{P}\exp\left(\frac{2B}{N_0}\right) + 1\right) \qquad (4.34a)$$

$$\mathrm{Var}\{\ln(L(\boldsymbol{y}; \mathcal{H}_0))\} \approx \ln\left(\frac{1 - \alpha}{P}\exp\left(\frac{2B}{N_0}\right) + 1\right), \qquad (4.34b)$$

where we can approximate, through (4.31),

$$\begin{aligned}\mathbb{E}\{\ln(L(\boldsymbol{y}; \mathcal{H}_0))\} &\approx -\frac{1}{2}\ln\left(\frac{1 - \alpha}{P}\exp\left(\frac{2B}{N_0}\right)\right) \\ &= \frac{1}{2}\ln\left(\frac{P}{1 - \alpha}\right) - \frac{B}{N_0} \qquad (4.35a) \\ \mathrm{Var}\{\ln(L(\boldsymbol{y}; \mathcal{H}_0))\} &\approx \ln\left(\frac{1 - \alpha}{P}\exp\left(\frac{2B}{N_0}\right)\right) \\ &= \frac{2B}{N_0} - \ln\left(\frac{P}{1 - \alpha}\right). \qquad (4.35b)\end{aligned}$$

These results apply also to $\mathbb{E}\{\ln(L(\boldsymbol{y}|p \leq C; \mathcal{H}_1))\}$ and $\mathrm{Var}\{\ln(L(\boldsymbol{y}|p \leq C; \mathcal{H}_1))\}$ as mentioned before.

If we take (4.18) for $A = 0$ we have

$$\mathbb{E}\{L(\boldsymbol{y}|p > C; \mathcal{H}_1)\} \approx \frac{1}{P}\left(P + \exp\left(\frac{2B^2}{N_0} - 1\right)\right) \tag{4.36a}$$

$$\begin{aligned}\mathrm{Var}\{L(\boldsymbol{y}|p > C; \mathcal{H}_1)\} \approx \frac{1}{P^2}\Bigg[&(P - C - 1)\left(\exp\left(\frac{2B^2}{N_0}\right) - 1\right) \\ &+ \left(\exp\left(\frac{2B^2}{N_0}\right) - 1\right)\exp\left(\frac{4B^2}{N_0}\right)\Bigg].\end{aligned} \tag{4.36b}$$

Considering the assumption (4.30) we can approximate (4.36) as

$$\mathbb{E}\{L(\boldsymbol{y}|p > C; \mathcal{H}_1)\} \approx \frac{1}{P}\left(P + \exp\left(\frac{2B^2}{N_0}\right)\right) \tag{4.37a}$$

$$\mathrm{Var}\{L(\boldsymbol{y}|p > C; \mathcal{H}_1)\} \approx \frac{1}{P^2}\left[(P - C - 1)\exp\left(\frac{2B^2}{N_0}\right) + \exp\left(\frac{6B^2}{N_0}\right)\right]. \tag{4.37b}$$

Then using (4.31) we get

$$\mathbb{E}\{L(\boldsymbol{y}|p > C; \mathcal{H}_1)\} \approx \frac{1}{P}\exp\left(\frac{2B^2}{N_0}\right) \tag{4.38a}$$

$$\mathrm{Var}\{L(\boldsymbol{y}|p > C; \mathcal{H}_1)\} \approx \frac{1}{P^2}\exp\left(\frac{6B^2}{N_0}\right). \tag{4.38b}$$

For the log-likelihood function, (4.21), we can again use (4.19)

$$\begin{aligned}\mathbb{E}\{\ln(L(\boldsymbol{y}|p > C; \mathcal{H}_1))\} \approx &\ln\left[\frac{1}{P}\exp\left(\frac{2B^2}{N_0}\right)\right] \\ &- \frac{1}{2}\ln\left[\exp\left(\frac{2B^2}{N_0}\right) + 1\right]\end{aligned} \tag{4.39a}$$

$$\mathrm{Var}\{\ln(L(\boldsymbol{y}|p > C; \mathcal{H}_1))\} \approx \ln\left[\exp\left(\frac{2B^2}{N_0}\right) + 1\right]. \tag{4.39b}$$

Assuming once again (4.30) and (4.31)

$$\begin{aligned}\mathbb{E}\{\ln(L(\boldsymbol{y}|p>C;\mathcal{H}_1))\} &\approx \frac{2B^2}{N_0} - \ln(P) - \frac{B^2}{N_0} \\ &= \frac{B^2}{N_0} - \ln(P) \end{aligned} \tag{4.40a}$$

$$\mathrm{Var}\{\ln(L(\boldsymbol{y}|p>C;\mathcal{H}_1))\} \approx \frac{2B^2}{N_0}. \tag{4.40b}$$

So we have obtained through approximation fairly simple expressions to characterize the statistics of the log-likelihood function for the different cases. We can now plug these expressions in (4.24) where we can notice that since the statistics for $\mathcal{H}_0$ coincide with the ones for $\mathcal{H}_1$ and $p \leq C$ the first part simplifies to P_{FA}

$$\begin{aligned} P_{\mathrm{D}} &= \alpha P_{\mathrm{FA}} + (1-\alpha) \\ &\quad \times \mathrm{Q}\left[\frac{\sqrt{\frac{2B^2}{N_0} - ln(\frac{P}{1-\alpha})}\mathrm{Q}^{-1}(P_{\mathrm{FA}}) + \frac{1}{2}\ln\left(\frac{P}{1-\alpha}\right) - \frac{2B^2}{N_0} + \ln(P)}{\sqrt{\frac{2B^2}{N_0}}}\right] \\ &= \alpha P_{\mathrm{FA}} + (1-\alpha)\,\mathrm{Q}\left[\sqrt{1 - \frac{N_0}{2B^2}\ln\left(\frac{P}{1-\alpha}\right)}\mathrm{Q}^{-1}(P_{\mathrm{FA}})\right. \\ &\quad \left. - \sqrt{\frac{2B^2}{N_0}} + \frac{1}{2}\sqrt{\frac{N_0}{2B^2}}\ln\left(\frac{P^3}{1-\alpha}\right)\right]. \end{aligned} \tag{4.41}$$

The last step would be to rearrange the expression using (4.29)

$$\begin{aligned} P_{\mathrm{D}} = \alpha P_{\mathrm{FA}} + (1-\alpha)\,\mathrm{Q}\left[\sqrt{1 - \frac{1-\alpha}{\mathrm{SNR}}\ln\left(\frac{P}{1-\alpha}\right)}\mathrm{Q}^{-1}(P_{\mathrm{FA}})\right. \\ \left. -\sqrt{\frac{\mathrm{SNR}}{1-\alpha}} + \frac{1}{2}\sqrt{\frac{1-\alpha}{\mathrm{SNR}}}\ln\left(\frac{P^3}{1-\alpha}\right)\right]. \end{aligned} \tag{4.42}$$

This formula will be useful for analyzing the scenario from a theoretical point of view and get further understanding of the problem.

4.3.3 Validation of the approximation

So as to know how well our approximations perform we will compare the approximated formula with the original formula. We will also check with the simulation results, although in this case we will take the assumptions that $A = 0$, that the power of the channel is just 1 and that the SNR is defined as in (4.29). Therefore,

each ROC curve obtained will just depend on the SNR, the P value and the α value.

In Figures 4.11-4.20 we can see the ROC curves for the simulated, calculated and approximated results. We can see that, in general, the approximation (4.42) gets almost the same ROC curves as the the original formula (4.24), and thus, it is the previous characterization that limits the applicability of our final formula. However, if we look at Figure 4.18 we see a small error between the approximation and the original formula. This is because in our approximation we are using directly the value α without computing $C = \alpha P$, which has to be an integer, and so it is rounded to the nearest one. Therefore, if we use a P which is too small to ignore this fact, and such that αP doesn't give an integer value we can have this problem, but we will be working with large enough P values so this shouldn't pose a problem.

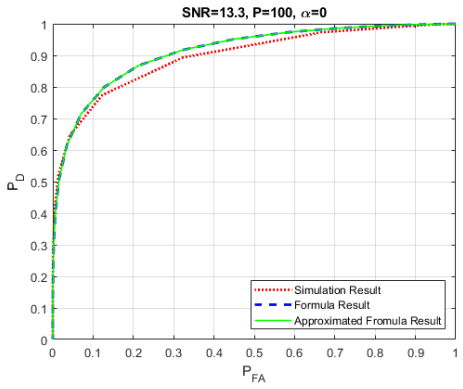

Figure 4.11: Simulated, calculated and approximated ROC curves for $SNR = 13.3$, $P = 100$ and $\alpha = 0$.

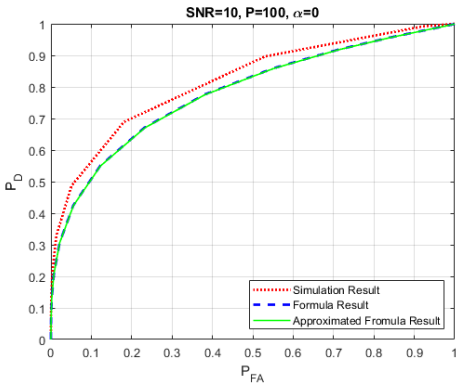

Figure 4.12: Simulated, calculated and approximated ROC curves for $SNR = 10$, $P = 100$ and $\alpha = 0$.

4.4 Interpretation of the Formula

After obtaining and approximated formula (4.42) for P_{D}, the problem is now to get some insight out of it. We can easily see that the P_{D} grows with SNR, as common sense would suggest, since the value inside the Q function gets more negative ($\mathrm{Q}(x)$ is decreasing with x). We can also get an upper limit for the probability of detection in case Q gets to its maximum, 1. This would give us

$$P_{\mathrm{D}} \leq P_{\mathrm{Dmax}} = \alpha P_{\mathrm{FA}} + (1 - \alpha), \tag{4.43}$$

where the optimum is $\alpha = 0$, where we would get $P_{\mathrm{D}} = 1$. However, apart from these simple relations it is hard to see clear relations between P_{D} and the rest of the variables, specially α. A good way to get some more insight of these relations is to take derivatives with respect to α and analyze what we get.

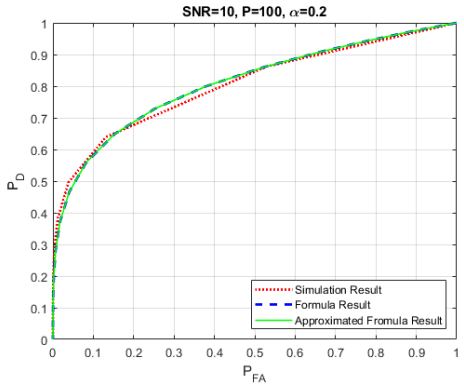

Figure 4.13: Simulated, calculated and approximated ROC curves for $SNR = 10$, $P = 100$ and $\alpha = 0.2$.

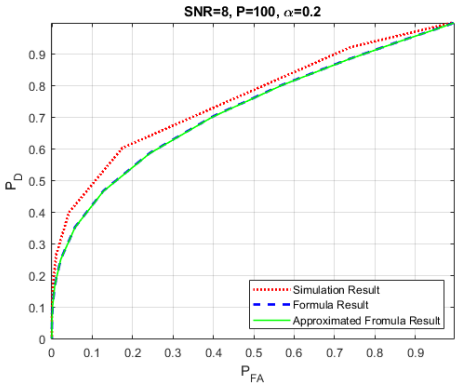

Figure 4.14: Simulated, calculated and approximated ROC curves for $SNR = 8$, $P = 100$ and $\alpha = 0.2$.

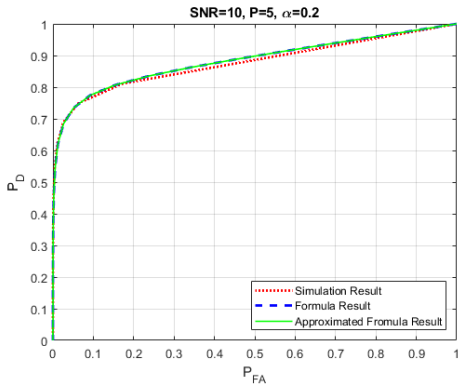

Figure 4.15: Simulated, calculated and approximated ROC curves for $SNR = 10$, $P = 5$ and $\alpha = 0.2$.

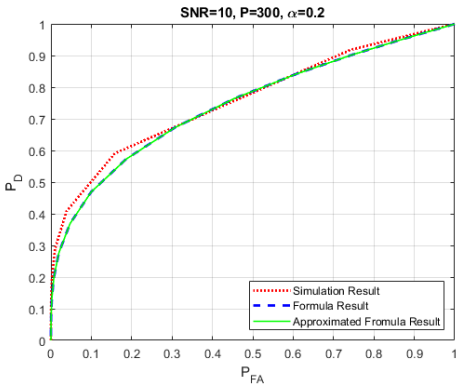

Figure 4.16: Simulated, calculated and approximated ROC curves for $SNR = 10$, $P = 300$ and $\alpha = 0.2$.

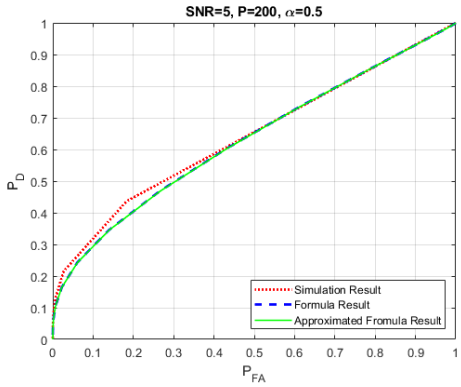

Figure 4.17: Simulated, calculated and approximated ROC curves for $SNR = 5$, $P = 200$ and $\alpha = 0.5$.

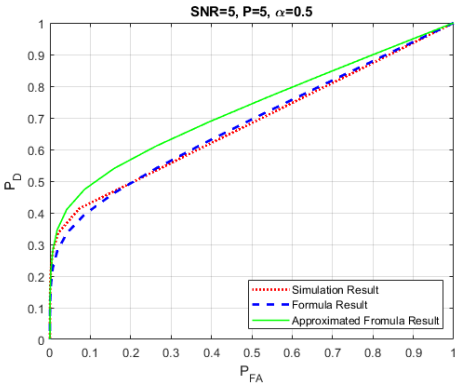

Figure 4.18: Simulated, calculated and approximated ROC curves for $SNR = 5$, $P = 5$ and $\alpha = 0.5$.

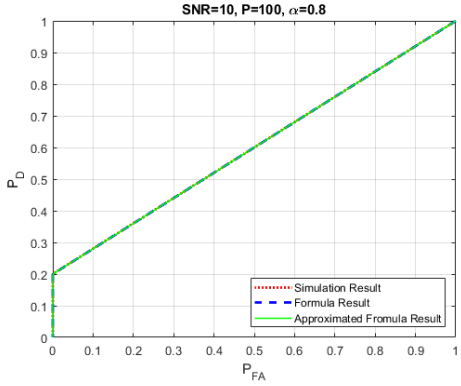

Figure 4.19: Simulated, calculated and approximated ROC curves for $SNR = 10$, $P = 100$ and $\alpha = 0.8$.

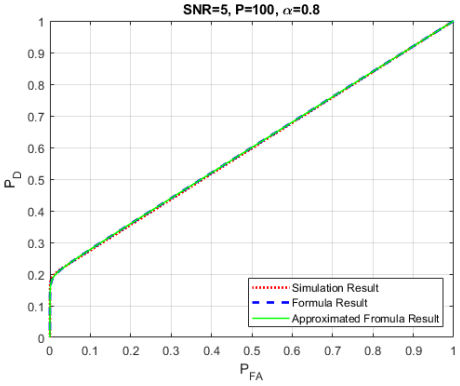

Figure 4.20: Simulated calculated and approximated ROC curves for $SNR = 5$, $P = 100$ and $\alpha = 0.8$ and $\alpha = 0$.

4.4.1 Differentiation with respect to α

In Figures 4.21, 4.22 and 4.23 we have some examples of how would the P_{D} over α look like depending on the properties of its derivatives that we could expect. If

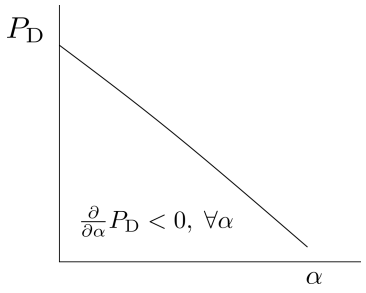

Figure 4.21: Example of P_{D} over α with negative first derivative.

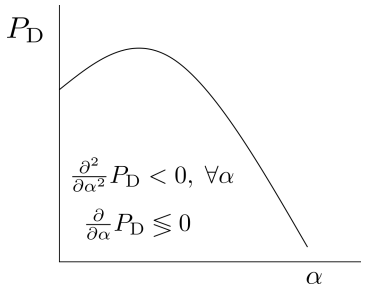

Figure 4.22: Example of P_{D} over α with negative second derivative.

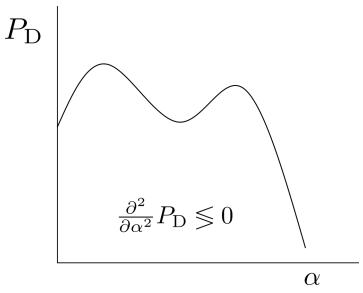

Figure 4.23: Example of P_{D} over α with unconstrained derivatives.

we take the first derivative of the P_{D} in (4.42) with respect to α we get

$$\frac{\partial}{\partial\alpha}P_{\mathrm{D}} = P_{\mathrm{FA}} + (1-\alpha)\frac{\partial \mathrm{Q}(g(\alpha))}{\partial\alpha} - \mathrm{Q}(g(\alpha)), \tag{4.44}$$

with

$$\begin{aligned} g(\alpha) = \sqrt{1 - \frac{(1-\alpha)}{\mathrm{SNR}}\ln\left(\frac{P}{(1-\alpha)}\right)}\mathrm{Q}^{-1}(P_{\mathrm{FA}}) - \sqrt{\frac{\mathrm{SNR}}{(1-\alpha)}} \\ + \frac{1}{2}\sqrt{\frac{(1-\alpha)}{\mathrm{SNR}}}\ln\left(\frac{P^3}{(1-\alpha)}\right), \end{aligned} \tag{4.45}$$

and where we have the problem of differentiating the special function $\mathrm{Q}(x)$. However, this function is just an integral of the form

$$\mathrm{Q}(x) = \frac{1}{\sqrt{2\pi}}\int_x^\infty \exp\left(-\frac{u^2}{2}\right)\mathrm{d}u. \tag{4.46}$$

Therefore, we can use the Leibniz integral rule [22] that states

$$\frac{\mathrm{d}}{dx}\left(\int_{a(x)}^{b(x)} f(x,t)\mathrm{d}t\right) = f(x,b(x))\frac{\mathrm{d}}{\mathrm{d}x}b(x) - f(x,a(x))\frac{\mathrm{d}}{\mathrm{d}x}a(x) + \int_{a(x)}^{b(x)} \frac{\partial}{\partial x} f(x,t)\mathrm{d}t. \tag{4.47}$$

In our case, we can express $\frac{\partial \mathrm{Q}(g(\alpha))}{\partial \alpha}$ as

$$\begin{aligned} \frac{\partial \mathrm{Q}(g(\alpha))}{\partial \alpha} &= \frac{\partial}{\partial \alpha}\left(\frac{1}{\sqrt{2\pi}}\int_{g(\alpha)}^{\infty} \exp\left(-\frac{u^2}{2}\right)\mathrm{d}u\right) \\ &= -\frac{1}{\sqrt{2\pi}}\exp\left(-\frac{g(\alpha)^2}{2}\right)\frac{\partial g(\alpha)}{\partial \alpha}, \end{aligned} \tag{4.48}$$

where we just need to calculate the derivative of $g(\alpha)$ which gives

$$\begin{aligned} \frac{\partial g(\alpha)}{\partial \alpha} &= \frac{\ln(\frac{P}{1-\alpha}) - 1}{2\mathrm{SNR}\sqrt{1 - \frac{(1-\alpha)}{\mathrm{SNR}}\ln\left(\frac{P}{1-\alpha}\right)}}\mathrm{Q}^{-1}(P_{\mathrm{FA}}) - \frac{\ln\left(\frac{P^3}{1-\alpha}\right)}{4\mathrm{SNR}\sqrt{\frac{1-\alpha}{\mathrm{SNR}}}} \\ &\quad + \frac{1}{2(1-\alpha)}\sqrt{\frac{1-\alpha}{\mathrm{SNR}}}\left(1 - \frac{\mathrm{SNR}}{1-\alpha}\right) \\ &= \frac{\ln\left(\frac{P}{1-\alpha}\right) - 1}{2\mathrm{SNR}\sqrt{1 - \frac{(1-\alpha)}{\mathrm{SNR}}\ln\left(\frac{P}{1-\alpha}\right)}}\mathrm{Q}^{-1}(P_{\mathrm{FA}}) \\ &\quad + \frac{1}{2\sqrt{\mathrm{SNR}(1-\alpha)}}\left(1 - \frac{\mathrm{SNR}}{1-\alpha} - \frac{\ln\left(\frac{P^3}{1-\alpha}\right)}{2}\right). \end{aligned} \tag{4.49}$$

Having characterized $\frac{\partial}{\partial \alpha}P_{\mathrm{D}}$, we know that if this derivative is always negative then the optimum α would just be 0. Another possibility is that, if we can prove that the second derivative is always negative, it is enough to evaluate the first derivative at the point $\alpha = 0$ to see if there would be a maximum α different from 0 (in case this derivative is positive) or if the optimum α is 0 (in case this derivative is negative). So if we take the second derivative over P_{D} we have

$$\begin{aligned} \frac{\partial^2}{\partial \alpha^2}P_{\mathrm{D}} &= \frac{\partial}{\partial \alpha}\left(P_{\mathrm{FA}} + (1-\alpha)\frac{\partial \mathrm{Q}(g(\alpha))}{\partial \alpha} - \mathrm{Q}(g(\alpha))\right) \\ &= (1-\alpha)\frac{\partial^2 \mathrm{Q}(g(\alpha))}{\partial \alpha^2} - 2\frac{\partial \mathrm{Q}(g(\alpha))}{\partial \alpha}, \end{aligned} \tag{4.50}$$

where we just need to calculate $\frac{\partial^2 \mathrm{Q}(g(\alpha))}{\partial \alpha^2}$ since we already have the rest. We can express this second derivative as

$$\begin{aligned}\frac{\partial^2 \mathrm{Q}(g(\alpha))}{\partial \alpha^2} &= \frac{\partial}{\partial \alpha}\left(-\frac{1}{\sqrt{2\pi}}\exp\left(-\frac{g(\alpha)^2}{2}\right)\frac{\partial g(\alpha)}{\partial \alpha}\right) \\ &= \frac{1}{\sqrt{2\pi}}\exp\left(-\frac{g(\alpha)^2}{2}\right)\left(g(\alpha)\left(\frac{\partial g(\alpha)}{\partial \alpha}\right)^2 - \frac{\partial^2 g(\alpha)}{\partial \alpha^2}\right), \quad (4.51)\end{aligned}$$

and where again we already know everything except for $\frac{\partial^2 g(\alpha)}{\partial \alpha^2}$, which can be obtained differentiating (4.49) as

$$\begin{aligned}\frac{\partial^2 g(\alpha)}{\partial \alpha^2} &= \mathrm{Q}^{-1}(P_{\mathrm{FA}}) \\ &\quad \times \frac{\frac{2}{1-\alpha}\mathrm{SNR}\sqrt{1-\frac{(1-\alpha)}{\mathrm{SNR}}\ln\left(\frac{P}{1-\alpha}\right)} - \left(\ln\left(\frac{P}{1-\alpha}\right)\right)\left(\ln\left(\frac{P}{(1-\alpha)}\right)-1\right)}{2\mathrm{SNR}\sqrt{1-\frac{1-\alpha}{\mathrm{SNR}}\ln\left(\frac{P}{1-\alpha}\right)}} \\ &\quad + \frac{2\sqrt{(1-\alpha)\mathrm{SNR}}\left(-\frac{\mathrm{SNR}}{(1-\alpha)^2}-\frac{1}{2(1-\alpha)}\right)+\mathrm{SNR}\left(1-\frac{\mathrm{SNR}}{1-\alpha}-\frac{\ln\left(\frac{P^3}{1-\alpha}\right)}{2}\right)}{4\sqrt{\left((1-\alpha)\mathrm{SNR}\right)^3}} \\ &= \frac{\mathrm{Q}^{-1}(P_{\mathrm{FA}})}{2\mathrm{SNR}(1-\alpha)\sqrt{1-\frac{(1-\alpha)}{\mathrm{SNR}}\ln\left(\frac{P}{1-\alpha}\right)}}\left(1-\frac{(1-\alpha)\left(\ln\left(\frac{P}{1-\alpha}\right)-1\right)^2}{2\mathrm{SNR}\left(1-\frac{1-\alpha}{\mathrm{SNR}}\ln\left(\frac{P}{1-\alpha}\right)\right)}\right) \quad (4.52) \\ &\quad - \frac{6\mathrm{SNR}+(1-\alpha)\ln\left(\frac{P^3}{1-\alpha}\right)}{8(1-\alpha)^2\sqrt{(1-\alpha)\mathrm{SNR}}}.\end{aligned}$$

As it can be seen, the expressions obtained are not straightforward to analyze without taking further assumptions or computing them numerically for different cases. If we compute P_D with respect to α for a given P_{FA}, let's say $P_{\mathrm{FA}} = 10^{-3}$ since we are interested in low false alarm probabilities, we can get insights on how to optimize α for different SNR values. This relates with the results from the previous chapter, where the maximum loss optimization would correspond in the extreme case to set α to 0 by decreasing the maximum gain (yet maintaining the same L_{avg}).

If we look at Figure 4.24, where the value of SNR has been chosen as the limit where our approximated formula (4.42) is close to the simulations, we notice that the optimum α is not 0. However, if we increase the SNR, in Figure 4.25 we see that the optimum α is 0 in this case, and can see that the relation between P_{D} and α is almost linear. This suggests us that, if we go to the asymptotically high SNR

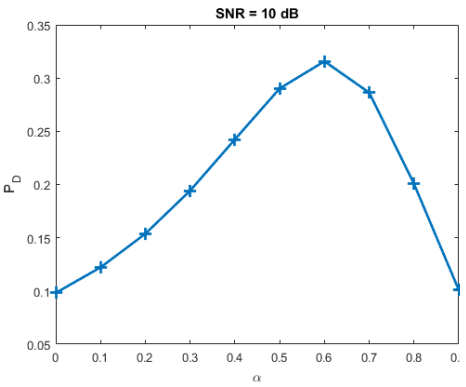

Figure 4.24: P_{D} over α for $P_{\mathrm{FA}} = 10^{-3}$, $P = 100$ and $\mathrm{SNR} = 10dB$ using the approximated formula.

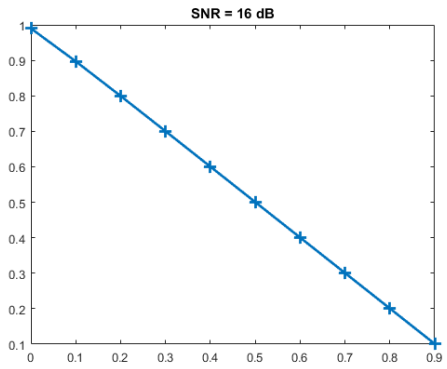

Figure 4.25: P_{D} over α for $P_{\mathrm{FA}} = 10^{-3}$, $P = 100$ and $\mathrm{SNR} = 16dB$ using the approximated formula.

region, $\frac{\partial}{\partial\alpha}P_{\mathrm{D}}$ will tend to be a negative constant. Thus, $\frac{\partial^2}{\partial\alpha^2}P_{\mathrm{D}}$ will tend to 0, and the optimum α will be always 0. Our main interest is to get closed form results, and the low SNR case appears to be too complicated to get them. Therefore, due to the intuition we get from Figure 4.25, we would like to explore in more detail the high SNR region to be able to get a better understanding of our results.

4.4.2 Asymptotic analysis

We want to find the limit of our formulas if we go to the asymptotically high SNR regime. However, it is of interest to analyze what happens if the constant P, which can be seen as the angular resolution in our original scenario, goes high too. By looking at (4.42), as well as at the expressions obtained for the the different derivatives, we notice that there are many fractions of the form $\frac{\ln(P)}{\mathrm{SNR}}$, so it can be of interest to take both the SNR and the $\ln(P)$ to infinity at a constant rate

$$\left.\frac{\ln(P)}{\mathrm{SNR}}\right|_{\substack{P\to\infty \\ \mathrm{SNR}\to\infty}} = \beta, \tag{4.53}$$

and get the asymptotic results. Note that, considering (4.31), β has to be at least lower than 1 for our approximations to hold, and that we could compute the limit of the SNR going to infinity for a finite P if we set $\beta = 0$.

Due to the complexity of the final expressions we are going to go step by step, but a reader not interested in these derivations can continue from (4.60).

If we assume (4.53) in (4.45) we get

$$\begin{aligned} g(\alpha)\Big|_{\substack{P\to\infty \\ \mathrm{SNR}\to\infty}} &= \sqrt{1-(1-\alpha)\beta}\,\mathrm{Q}^{-1}(P_{\mathrm{FA}}) - \sqrt{\frac{\mathrm{SNR}}{(1-\alpha)}} \\ &\quad + \frac{3}{2}\sqrt{(1-\alpha)\mathrm{SNR}}\,\beta \\ &= \sqrt{\frac{\mathrm{SNR}}{1-\alpha}}\left(\frac{3\beta(1-\alpha)}{2} - 1\right). \end{aligned} \tag{4.54}$$

Note that this expression can either go to $+\infty$ or $-\infty$ depending on the sign of $\left(\frac{3\beta(1-\alpha)}{2} - 1\right)$. We do the same for (4.49)

$$\begin{aligned} \frac{\partial g(\alpha)}{\partial \alpha}\Big|_{\substack{P\to\infty \\ \mathrm{SNR}\to\infty}} &= \frac{\beta}{2\sqrt{1-(1-\alpha)\beta}}\mathrm{Q}^{-1}(P_{\mathrm{FA}}) \\ &\quad + \sqrt{\frac{\mathrm{SNR}}{1-\alpha}}\left(\frac{1}{\sqrt{\mathrm{SNR}}} - \frac{1}{1-\alpha} - \frac{3\beta}{2}\right) \\ &= -\frac{1}{2}\sqrt{\frac{\mathrm{SNR}}{1-\alpha}}\left(\frac{1}{1-\alpha} + \frac{3\beta}{2}\right), \end{aligned} \tag{4.55}$$

where in this case the result will always tend to $-\infty$ no matter the value of β we choose. For (4.52) we have

$$\begin{aligned} \frac{\partial^2 g(\alpha)}{\partial \alpha^2}\Big|_{\substack{P\to\infty \\ \mathrm{SNR}\to\infty}} &= \frac{\mathrm{Q}^{-1}(P_{\mathrm{FA}})}{4(1-\alpha)\sqrt{1-(1-\alpha)\beta}}\left(\frac{(1-\alpha)\beta^2}{(1-(1-\alpha)\beta)}\right) \\ &\quad - \sqrt{\frac{\mathrm{SNR}}{(1-\alpha)^3}}\frac{6+(1-\alpha)3\beta}{8} \\ &= -\sqrt{\frac{\mathrm{SNR}}{(1-\alpha)^3}}\frac{6+(1-\alpha)3\beta}{8}, \end{aligned} \tag{4.56}$$

where again this result will tend to $-\infty$ regardless of the value of β. Now we can use these results in (4.48) and (4.51) getting

$$\begin{aligned} \frac{\partial \mathrm{Q}(g(\alpha))}{\partial \alpha}\Big|_{\substack{P\to\infty \\ \mathrm{SNR}\to\infty}} &= \frac{1}{\sqrt{2\pi}}\exp\left(-\frac{\frac{\mathrm{SNR}}{1-\alpha}\left(\frac{3\beta(1-\alpha)}{2} - 1\right)^2}{2}\right) \\ &\quad \times \frac{1}{2}\sqrt{\frac{\mathrm{SNR}}{1-\alpha}}\left(\frac{1}{1-\alpha} + \frac{3\beta}{2}\right) \\ &= 0, \end{aligned} \tag{4.57}$$

since the exponential of -SNR goes to 0 much faster than $\sqrt{\mathrm{SNR}}$ goes to ∞. For

(4.51) we have a similar case

$$\begin{aligned}\left.\frac{\partial^2 \mathrm{Q}(g(\alpha))}{\partial\alpha^2}\right|_{\substack{P\to\infty\\ \mathrm{SNR}\to\infty}} &= \frac{1}{\sqrt{2\pi}}\exp\left(-\frac{\frac{\mathrm{SNR}}{1-\alpha}\left(\frac{3\beta(1-\alpha)}{2}-1\right)^2}{2}\right)\\ &\quad\times\left(\sqrt{\left(\frac{\mathrm{SNR}}{1-\alpha}\right)^3}\left(\frac{3\beta(1-\alpha)}{2}-1\right)\left(\frac{1}{1-\alpha}+\frac{3\beta}{2}\right)^2\right.\\ &\quad\left.+\sqrt{\frac{\mathrm{SNR}}{(1-\alpha)^3}}\frac{6+(1-\alpha)3\beta}{8}\right)\\ &= 0, \end{aligned} \tag{4.58}$$

where in this case the exponential of $-\mathrm{SNR}$ still goes to 0 much slower than $\sqrt{\mathrm{SNR}^3}$ goes to infinity. We can also compute the limit for $\mathrm{Q}(g(\alpha))$ which gives

$$\left.\mathrm{Q}(g(\alpha))\right|_{\substack{P\to\infty\\ \mathrm{SNR}\to\infty}} = \begin{cases} 1 & \text{if} \quad \beta < \frac{2}{3(1-\alpha)} \\ 0 & \text{if} \quad \beta > \frac{2}{3(1-\alpha)}. \end{cases} \tag{4.59}$$

Using (4.57) and (4.58) in (4.50) we get

$$\left.\frac{\partial^2}{\partial\alpha^2}P_{\mathrm{D}}\right|_{\substack{P\to\infty\\ \mathrm{SNR}\to\infty}} = 0. \tag{4.60}$$

This means that, as we expected from Figure 4.25, if we increase sufficiently the SNR, the second derivative of P_{D} goes to 0. So if the first derivative at $\alpha = 0$ is negative then it would be optimum to choose $\alpha = 0$. If we use now the results in (4.44) we have

$$\left.\frac{\partial}{\partial\alpha}P_{\mathrm{D}}\right|_{\substack{P\to\infty\\ \mathrm{SNR}\to\infty}} = \begin{cases} P_{\mathrm{FA}} - 1 & \text{if} \quad \beta < \frac{2}{3(1-\alpha)} \\ P_{\mathrm{FA}} & \text{if} \quad \beta > \frac{2}{3(1-\alpha)}, \end{cases} \tag{4.61}$$

where we can note that P_{FA} is a value between 0 and 1 (and we are interested in the region near 0), so $P_{\mathrm{FA}} - 1$ will be a negative constant and P_{FA} will be a positive constant. If we take $\alpha = 0$ we have

$$\left.\frac{\partial}{\partial\alpha}P_{\mathrm{D}}\right|_{\substack{P\to\infty\\ \mathrm{SNR}\to\infty}} = \begin{cases} P_{\mathrm{FA}} - 1 & \text{if} \quad \beta < \frac{2}{3} \\ P_{\mathrm{FA}} & \text{if} \quad \beta > \frac{2}{3}. \end{cases} \tag{4.62}$$

This means that, if $\beta > \frac{2}{3}$, the first derivative of P_{D} is negative at $\alpha = 0$ while the second derivative is always 0, so the maximum P_{D} is found at $\alpha = 0$. On the other hand, if $\beta < \frac{2}{3}$, the first derivative of P_{D} is positive at $\alpha = 0$ while the second derivative is still 0, so it is optimum to choose α as close as possible to 1 (note that it cannot be 1 since it would mean that we are not receiving anything at all).

At this point we should consider the meaning of β. In a normal scenario β will be a really small number since increasing P exponentially with relation to the SNR appears to be unreasonable; if we see P as the precision it would be the same as saying that we are increasing the precision with the exponential of the SNR. In reality the precision will be fixed and limited by other factors so that β will in general be smaller that $\frac{2}{3}$.

4.5 Concluding remarks

Through this chapter we have defined a simple scenario to be able to get understanding of our original problem. We have characterized the scenario by obtaining an approximated formula and we have been able to get closed form results in the asymptotically high SNR region.

Taking the asymptotic results and with the consideration that β will be in general smaller than $\frac{2}{3}$ we can see that the best option is to set $\alpha = 0$ if the SNR is sufficiently high. This can be related to our original problem, in which we were trying to optimize the maximum loss, $L_{\max}$, and the average loss, L_{avg}. In this case L_{avg} is fixed and we can see that the best option, with the previous considerations, is to have the same gain all throughout the defined space instead of focusing just in some areas and get a higher gain there. So if we optimize the $L_{\max}$ using pure phase optimization we will have better detection performance considering that we have a sufficiently high SNR. Furthermore, the steering optimization results will have worse detection performance since they have in general a higher $L_{\max}$.

Chapter 5
Conclusions and Future Work

5.1 Conclusions

Throughout this thesis we have studied the possibilities of UE beamforming through a codebook approach in which the UE can only do beamforming using a closed set of phase combinations. We have obtained optimum codebooks for the metrics L_{avg} and $L_{\max}$ that we have defined. Optimizing these metrics can be helpful in 5G scenarios such as the initial discovery of the UE and the BS. For the optimization we have considered two approaches: steering optimization and pure phase optimization. The steering optimization defines the phase codebook in such a way that each codeword corresponds to steer the antenna at the UE to a certain direction. The pure phase optimization puts no constraint io the phase codebook so that the radiantion pattern of the antenna array at the UE for a given codeword don't necessarily have to point to a certain direction.

The optimized codebooks obtained have been utilized to analyze the estimation of the AoA at which an a signal coming from a BS is arriving the UE. The simulations showed that the pure phase optimized codebooks didn't have a clear improvement in terms of MSE for the AoA estimation. However, we noticed that the pure phase optimized codebooks performed better in detecting if a signal is being received or not (specialy the one optimizing $L_{\max}$), which is a necessary step before performing the AoA estimation.

We have also carried out a theoretical analysis to understand the influence of $L_{\max}$ in the detection performance. After an asymptotic analysis we have concluded that in the high SNR region it is best to optimize the metric $L_{\max}$ in terms of detection performance.

5.2 Future Work

The utilization of the antennas in the 5G UEs is still in need of deep research. The results from this thesis can be helpful for understanding some of the possibilities that utilizing these antennas offer. Some ideas for future research include the development of algorithms for the UE discovery, the construction of testbeds for testing these algorithms, the definition of the transmission and reception operating modes of the UEs, etc.

We can also think of future work more closely related to the results of this thesis. It would be interesting for example to look at the CRLB of the AoA estimation with respect to the phase codebook. This way we could obtain a direct way to optimize the phase codebooks this time in terms of MSE in the AoA estimation. Another suggested work is to calculate the AoA estimation performance when the signal is detected for a given P_{FA}, thus, considering the estimation problem and the detection problem altogether.

References

[1] J. G. Andrews et al., "What will 5G be?," *IEEE J. Sel. Areas Commun.*, vol. 32, no. 6, pp. 1065-1082, Jun. 2014.

[2] M. Agiwal et al., "Next generation 5G wireless networks: A comprehensive survey," *IEEE Commun. Surv. Tuts.*, vol. 18, no. 3, pp. 1617-1655, Third Quart. 2016.

[3] 3GPP TS 38.211-TS 38.214, 2018. [Online]. Available: `https://portal.3gpp.org/Specifications.aspx?q=1&releases=190`

[4] T. S. Rappaport et al., "Millimeter wave mobile communications for 5G cellular: It will work!," *IEEE Access*, vol. 1, pp. 335-349, May 2013.

[5] T. S. Rappaport et al., "Wideband millimiter-wave propagation: measurements and channel models for future wireless communication system design," *IEEE Trans. Commun.*, vol. 63, no. 9, pp.3029-3056, Sep. 2015.

[6] F. Rusek et al., "Scaling up MIMO: Opportunities and challenges with very large arrays," *IEEE Signal Process. Mag.*, vol. 30, no. 1, pp. 40-60, Jan. 2013.

[7] A. L. Swindlehurst et al., "Millimiter-wave massive MIMO: The next wireless revolution," *IEEE Commun. Mag.*, vol. 52, no. 9, pp. 56-62, Sep. 2014.

[8] T. L. Marzetta, "Noncooperative cellular wireless with unlimited numbers of base station antennas," *IEEE Trans. Wireless Commun.*, vol. 9, no. 11, Nov. 2011.

[9] B. Schulz, "LTE transmission modes and beamforming," Rhode and Schwarz, White Paper, Jul. 2011.

[10] Y. Huo et al., "5G cellular user equipment: From theory to practical hardware design," *IEEE Access*, vol. 5, pp. 13992-14010, Jul. 2017.

[11] 3GPP TS 38.101-4, "User Equipment (UE) radio transmission and reception; part 4: Performance requirements (rel. 15)," 2018. [Online]. Available: `http://www.3gpp.org/DynaReport/38101-4.htm`

[12] V. Raghavan et al., "Beamforming tradeoffs for initial UE discovery in millimeter-wave MIMO systems," *IEEE J. Sel. Topics Signal Process.*, vol. 10, no. 3, pp. 543-559, Apr. 2016.

[13] F. Sohrabi, and W. Yu, "Hybrid digital and analog beamforming design for large-scale antenna arrays," *IEEE J. Sel. Topics Signal Process.*, vol. 10, no. 3, pp. 501-513, Apr. 2016.

[14] S. J. Orfanidis, *Electromagnetic Waves and Antennas* 2016. [Online]. Available: `http://eceweb1.rutgers.edu/~orfanidi/ewa/`

[15] N. Deligiannis, and S. Louvros. 2009. "Hybrid TOA-AOA location positioning rechniques in GSM networks," *Wireless Pers. Commun.*, vol. 54, pp. 321-348, Jul. 2010.

[16] H. Liu et al., "Survey of Wireless Indoor Positioning Techniques and Systems," *IEEE Trans. Syst., Man, Cybern. C. Appl. Rev.*, vol. 37, no. 6, pp. 1067-1080, Nov. 2007.

[17] X. Zhang et al., "Angle-of-arrival based beamforming for FDD massive MIMO," in *Proc. 49th Asilomar Conf. Signals, Syst. Comput.*, pp. 704-708, Nov. 2015.

[18] L. C. Godara, "Application of antenna arrays to mobile communications, Part II: Beam-forming and direction-of-arrival considerations". *Proc. IEEE*, vol. 85, no. 8, pp. 1195-1245, Aug. 1997.

[19] S. M. Kay, *Fundamentals of Statistical Signal Processing. Vol. I. Estimation Theory*. Englewood Cliffs, NJ: Prentice Hall, 1993.

[20] S. M. Kay, *Fundamentals of Statistical Signal Processing. Vol. II. Detection Theory*. Englewood Cliffs, NJ: Prentice Hall, 1998.

[21] L.F. Fenton, "The sum of log-normal probability distributions in scatter transmission systems," *IRE Tras. Commun.*, vol. COM-8, no.1, pp. 57-67, Mar. 1960.

[22] H. Flanders, "Differentiation under the integral sign," *The American Mathematical Monthly*, vol. 80, no.6, pp. 615-627, Jun.-Jul. 1973.